www.nature.com/mi

MucosalImmunology

ARTICLE

Dopaminergic signalling limits suppressive activity and gut homing of regulatory T cells upon intestinal inflammation

Valentina Ugalde[1], Francisco Contreras[1], Carolina Prado[1], Ornella Chovar[1], Alexandra Espinoza[1] and Rodrigo Pacheco[1,2]

Evidence from inflammatory bowel diseases (IBD) patients and animal models has indicated that gut inflammation is driven by effector CD4$^+$ T-cell, including Th1 and Th17. Conversely, Treg seem to be dysfunctional in IBD. Importantly, dopamine, which is abundant in the gut mucosa under homoeostasis, undergoes a sharp reduction upon intestinal inflammation. Here we analysed the role of the high-affinity dopamine receptor D3 (DRD3) in gut inflammation. Our results show that *Drd3* deficiency confers a stronger immunosuppressive potency to Treg, attenuating inflammatory colitis manifestation in mice. Mechanistic analyses indicated that DRD3-signalling attenuates IL-10 production and limits the acquisition of gut-tropism. Accordingly, the ex vivo transduction of wild-type Treg with a siRNA for *Drd3* induced a potent therapeutic effect abolishing gut inflammation. Thus, our findings show DRD3-signalling as a major regulator of Treg upon gut inflammation.

Mucosal Immunology (2021) 14:652–666; https://doi.org/10.1038/s41385-020-00354-7

INTRODUCTION

Inflammatory bowel diseases (IBD) are a group of chronic inflammatory disorders that affect the gastrointestinal tract, among which Crohn's disease (CD) and ulcerative colitis (UC) are the most common. Studies performed in UC and CD patients as well as in animal models have indicated that gut inflammation in IBD is driven mainly by Th1 and Th17 lymphocytes.[1,2] Moreover, Treg lymphocytes, a subset of T-cells that exert suppressive activity and play a fundamental role in maintaining intestinal homoeostasis in steady-state conditions, is dysfunctional in IBD.[3] The administration of exogenous Treg cells in mouse models of inflammatory colitis might suppress the inflammation exerted by Th1 and Th17 lymphocytes;[4–6] an effect that underlies on IL-10 and TGF-β secretion by these cells. Interestingly, the population of intestinal Treg has been shown enhanced in the lesioned mucosa of IBD patients in comparison to non-inflamed tissue and mucosa from healthy subjects. Furthermore, after their isolation from lesioned mucosa, these cells display normal suppressive activity in vitro,[7,8] thereby suggesting that Treg function is impaired just in situ by environmental mediators present in the inflamed gut mucosa.

Cells located in the gut mucosa are exposed to dopamine that can come from different sources, including some clostridial bacteria of the gut microbiota,[9,10] the intrinsic enteric nervous system, the intestinal epithelial layer,[11] and some cells of the immune system, including dendritic cells (DCs) and Treg.[12,13] Interestingly, gut inflammation in CD and UC patients involves an abrupt reduction in the levels of dopamine,[14] thereby affecting the behaviour of cells that express dopamine receptors (DRs), including Treg and effector T-cells. Of note, a decrease in the levels of mucosal dopamine has also been described in the intestine of animal models of inflammatory colitis,[11,15] resembling the situation observed in IBD.

Dopamine can stimulate five different DRs, termed DRD1-DRD5. CD4$^+$ T lymphocytes from both human and mouse have been found to express functional DRs.[16] Importantly, the DRs display a broad range of affinity for dopamine, from nM to μM, being DRD3 the receptor with the highest affinity (Ki = 27 nM).[11] Therefore, the functional relevance of each DR is dependent on the concentration of dopamine. Our previous studies addressing the role of DRs expressed in CD4$^+$ T-cells in inflammation have shown that *Drd3* deficiency in naive CD4$^+$ T-cells leads to impaired Th1 differentiation and attenuated expansion of Th17 cells, thereby dampening the severity of inflammatory colitis.[17,18] Considering the decrease of mucosal dopamine in the intestine (from ≈1000 nM in healthy subjects to ≈100 nM in IBD patients[10,14]) and that DRD3 might be selectively stimulated by low-dopamine levels,[19] our previous findings suggest that the low concentration of mucosal dopamine associated to gut inflammation evokes the inflammatory potential of CD4$^+$ T-cells, thus favouring chronic inflammation.

Emerging evidence indicates that high dopamine levels exert a strong anti-inflammatory effect in several animal models of inflammation by stimulating low-affinity dopamine receptors, including DRD1 and DRD2.[20–22] In this regard, high dopamine concentrations present in the intestinal mucosa of healthy subjects would lead to DRD1 stimulation in macrophages, attenuating the activation of the inflammasome NLRP3 and thereby abrogating the production of inflammatory cytokines.[21] Moreover, high levels of dopamine lead to DRD2 stimulation, which not only favours the production of IL-10 by CD4$^+$ T lymphocytes,[23] but also inhibits the increased motility and dampens ulcer development in the intestine.[24] In fact, a genetic polymorphism of the *DRD2* gene associated with decreased DRD2 expression has been identified as a risk factor for IBD.[25] Accordingly, a study in mice showed that despite the percentage of mucosal Treg lymphocytes did not change upon intestinal inflammation, their suppressive function was impaired,[3] a condition associated with reduced mucosal dopamine.[15] Moreover, the administration of a DRD2 agonist, cabergoline, rescued the

[1]Laboratorio de Neuroinmunología, Fundación Ciencia & Vida, 7780272 Ñuñoa, Santiago, Chile and [2]Universidad San Sebastián, 7510156 Providencia, Santiago, Chile
Correspondence: Rodrigo Pacheco (rpacheco@cienciavida.org)

Received: 31 January 2020 Revised: 9 October 2020 Accepted: 21 October 2020
Published online: 12 November 2020

suppressive activity of Treg lymphocytes.[3] Altogether, these findings suggest that DRD2-signalling in Treg cells favours the suppressive function in the intestinal mucosa containing high levels of dopamine.

Here we hypothesise that low-dopamine levels associated with inflammation should selectively stimulate DRD3-signalling in Treg, dampening their suppressive activity in the inflamed gut mucosa. Thus, we aimed to analyse the role of DRD3-signalling in the function of Treg cells using an animal model of inflammatory colitis. Our results revealed that DRD3-signalling in Treg cells attenuates their suppressive activity and strongly reduces their gut tropism. Accordingly, *Drd3*-deficient mice were refractory to the development of inflammatory colitis and the inhibition of DRD3-signalling in Treg cells induced a potent anti-inflammatory effect with therapeutic potential in gut inflammation.

RESULTS

Genetic *Drd3*-deficiency results in attenuated gut inflammation in a mouse model of inflammatory colitis

By using an animal model of inflammatory colitis induced by the transfer of naive $CD4^+$ T-cells into T-cell deficient mice, a model of inflammation that depends exclusively of T-cell response, our previous study show that *Drd3* deficiency in $CD4^+$ T-cells resulted in a significant attenuation in disease manifestation.[17] Despite in UC and CD T-cell response plays a central role driving gut-inflammation, cells of the innate immune system play also a relevant role contributing to the inflammatory process.[26] Since in human IBD both, the adaptive and the innate immune system contribute to the disease development, we sought to analyse the relevance of DRD3-signalling in a mouse model of inflammatory colitis induced by the administration of dextran sodium sulphate (DSS), a model that involves both, the innate and adaptive immune response.[27,28] To analyse the global role of DRD3-signalling in the development of inflammatory colitis, we first compared the development of inflammatory colitis induced by DSS in *Drd3*-sufficient and *Drd3*-deficient mice. Strikingly, the results show that *Drd3* deficiency resulted in a complete abrogation of disease manifestation, including the attenuation in the loss of body weight (Fig. 1a), which corresponds the main parameter to determine disease severity. An inhibited shortening of colon length (Fig. 1b) and attenuated inflammation in the gut mucosa as evidenced by histological analyses (Fig. 1c) were also observed in *Drd3*-deficient mice when compared with *Drd3*-sufficient mice. Because *Drd3* deficiency has been previously associated to behavioural alterations in mice, including depression and anxiety,[29] we tested whether differences in the loss of body weight observed between *Drd3*-sufficient and *Drd3*-deficient mice were due to an unequal consumption of drinking water upon the DSS treatment. The results show that water consumption was similar in both genotypes before and after starting the DSS-administration (Fig. 1d), thus ruling out the possibility that difference in body weight observed between wild-type and knockout mice was due to an unequal water consumption. Because DRD3 has been shown to be expressed not only in the adaptive immune system, but also in neutrophils, eosinophils and Natural Killer cells,[30] we next attempted to dissociate the relevance of DRD3-signalling in the adaptive immune system and outside the adaptive immune system in the development of inflammatory colitis. For this purpose, we crossed $Drd3^{-/-}$ mice with $Rag1^{-/-}$ mice to generate *Drd3*-deficient mice devoid of adaptive immune system. The results show that $Drd3^{-/-}$ $Rag1^{-/-}$ as well as $Drd3^{+/+}$ $Rag1^{-/-}$ mice were susceptible to develop DSS-induced inflammatory colitis and that both genotypes presented loss of body weight with similar intensity (Fig. S1), thus indicating that DRD3-signalling outside the adaptive immune system lacks relevance in the development of gut inflammation. Since the development of intestinal inflammation depends on the gut microbiota,[31] we next addressed the question of whether reduced manifestation of inflammatory colitis observed in *Drd3*-deficient mice was due to a different microbiota composition in comparison with *Drd3*-sufficent mice. For this purpose, we compared the development of DSS-inflammatory colitis in $Drd3^{+/+}$ and $Drd3^{-/-}$ mice that were previously co-housed or living in separated cages. The results show that *Drd3*-deficient mice were resistant to disease manifestation even after co-housed with *Drd3*-sufficient (Fig. S2). Similarly, $Drd3^{+/+}$ mice were susceptible to DSS-induced inflammatory colitis even when co-housed with $Drd3^{-/-}$ mice (Fig. S2). Thus, these results ruled out the possibility that decreased colitis manifestation observed in *Drd3*-deficient mice was due to their microbiota. Together, these results indicate that DRD3-signalling in the adaptive immune system plays an important role favouring the development of inflammatory colitis irrespective the microbiota composition.

Drd3 deficiency in Treg cells exacerbates their anti-inflammatory effect in inflammatory colitis

Our previous study shows that *Drd3* deficiency in naive $CD4^+$ T-cells, a subset devoid of Treg, results in a selective attenuation of Th1-mediated immunity, but not Th17-mediated reactions, in a model of antigen-specific immune response induced by the immunisation with the ovalbumin (OVA) derived peptide OT-II (pOTII, which corresponds to $OVA_{323-339}$).[17] Using the same antigen-specific immunisation model induced by pOTII, here we observed that *Drd3* deficiency in total $CD4^+$ T-cells, which includes the subset of Treg cells, results in impaired Th1- and Th17-mediated immunity (Fig. S3). Thus, together these results suggest that *Drd3* deficiency in Treg cells plays a relevant role in the control of Th17-mediated immunity. Of note, Th17-mediated immunity has been extensively involved in gut inflammation.[32,33]

To analyse the role of DRD3-signalling in Treg in the control of gut inflammation, we next aimed to determine DRD3 expression in Treg cells. For this purpose, the levels of *Drd3* transcripts were quantified in Treg differentiated in vitro from naive $CD4^+$ T-cells (iTreg) and generated in vivo (hereinafter called just Treg), which were isolated from the spleen or mesenteric lymph nodes (MLN). The results show that both iTreg and Treg display significant expression of *Drd3* transcripts, nevertheless the extent of *Drd3*-transcription was higher in Treg (Fig. S4A, B). Moreover, *Drd3*-mRNA expression was selectively increased in Treg, but not in conventional T-cells (Tconv), isolated from the MLN upon gut inflammation (Fig. S4C). According to these results, the surface expression of DRD3 was selectively increased in Treg cells obtained from the colonic lamina propria (cLP) upon gut inflammation (Fig. 2a and S5). To analyse whether DRD3-signalling was relevant in the generation of Treg, we next conducted experiments to determine the impact of *Drd3* deficiency in the in vitro differentiation of naive $CD4^+$ T-cells into iTregs and in the generation of Treg in vivo isolated from the spleen. The results show a similar extent of iTreg generation when compared the in vitro differentiation of *Drd3*-sufficient and *Drd3*-deficient naive $CD4^+$ T-cells (Fig. S6A). Similarly, no differences were detected in the frequency of Treg in the spleen of *Drd3*-sufficient and *Drd3*-deficient mice (Fig. S6B). Thus, these results suggest that DRD3-signalling does not play a relevant role in the generation of Treg cells.

To determine the relevance of DRD3-signalling in the suppressive potential of Treg in inflammatory colitis, we next evaluated the extent of disease manifestation in DSS-treated mice that received the adoptive transfer of *Drd3*-sufficient or *Drd3*-deficient Treg cells. Since we expected to observe a higher therapeutic effect in mice receiving *Drd3*-deficient Treg cells, considering a previous study[6] we transferred a suboptimal amount of Treg (3×10^5 cells per mouse). According to our hypothesis, whereas *Drd3*-sufficient Treg did not exert a significant therapeutic effect in the development of inflammatory colitis, mice receiving the transfer

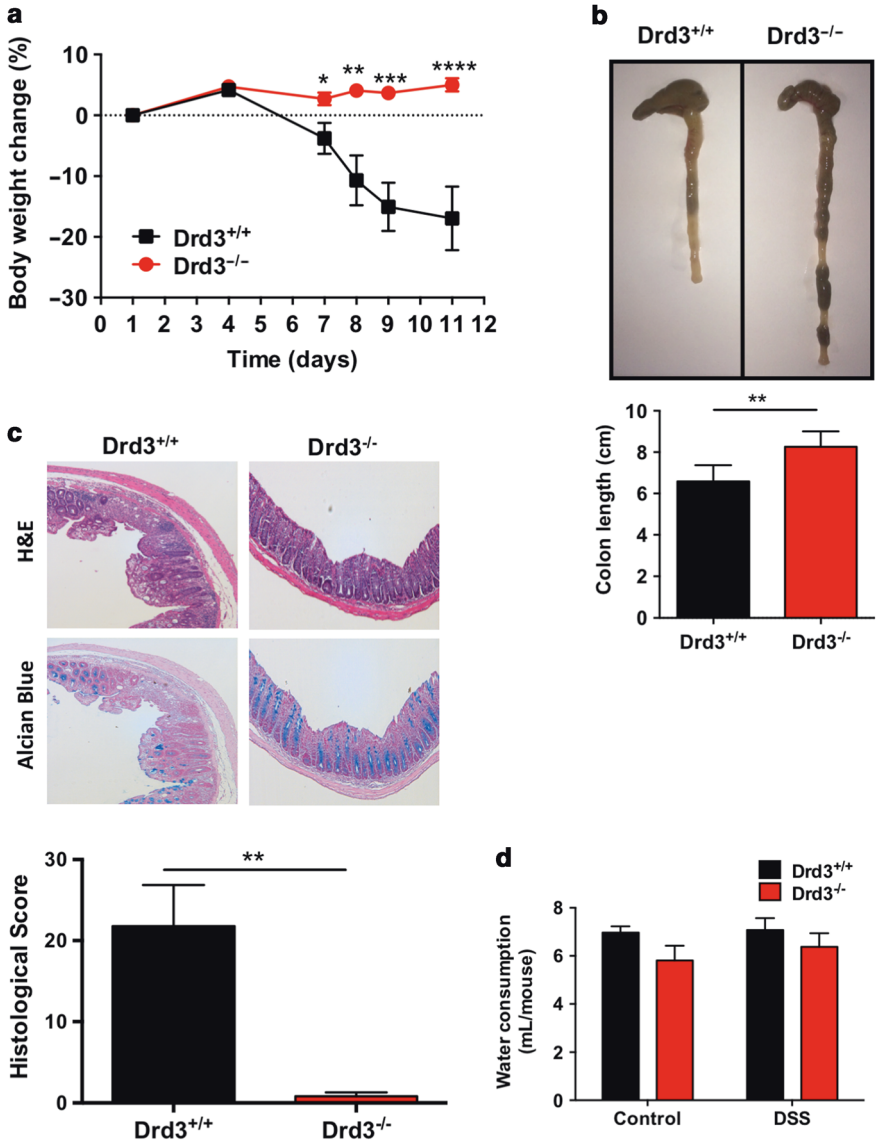

Fig. 1 ***Drd3*-deficient mice are unresponsive to DSS-induced inflammatory colitis.** *Drd3*$^{+/+}$ and *Drd3*$^{-/-}$ mice were exposed to 1% DSS in the drinking water for 8 days and then switched to normal water and monitored for 3 additional days. **a** Body weight was periodically registered throughout the whole time and the percentage of body weight change relative to initial weight was quantified. **b** On day 11, mice were sacrificed and the colon length was determined. Top panel shows representative images of a colon obtained from each experimental group. Bottom panel shows the quantification. **c** Histological analysis. Top panel shows representative images of H&E staining (top images) and alcian blue staining (bottom images) of distal colon sections. Bottom panel shows the quantification of histopathological score. **d** Water consumption was monitored during 3 days either before or during DSS treatment. Data correspond to the volume of water consumed per mice. **a**–**d** Values are expressed as mean ± SEM. Data from 7 (**a**, **b** and **d**) or 5 (**c**) mice per group are shown. Two independent experiments gave similar results. *$p < 0.05$; **$p < 0.01$; ***$p < 0.001$; ****$p < 0.0001$ by multiple Student's *t* test. No significant differences were found in **d** after the analysis by two-way ANOVA followed by Tukey's *post-hoc* test.

of *Drd3*-deficient Treg displayed a strong attenuation in the loss of body weight (Fig. 2b) and in the histopathological manifestation (Fig. 2c).

To evaluate the effect of DRD3-signalling in Treg cells in the control of inflammatory effector T-cell subsets in the colon and gut-associated lymphoid tissues (GALT), we analysed the frequency of relevant T-helper cells in the cLP and MLN of DSS-treated mice. Interestingly, the results show a selective reduction of Th17 frequency in MLN in mice receiving Treg transfer of both genotype (Fig. 2d). Nevertheless, mice receiving *Drd3*-deficient Treg show a more significant reduction in Th17 frequency than that observed in mice receiving *Drd3*-sufficient Treg cells (Fig. 2d). On the other hand, mice receiving the transfer or wild-type or knockout Treg displayed a strong and selective reduction of Th1 frequency in the cLP (Fig. 2e). Altogether these results suggest that DRD3-signalling in Treg plays a relevant role limiting their suppressive activity. Because the $CD3^+CD4^+CD25^+$ subset of T-cells (used in Fig. 2b as Treg) might contain not only Treg but also some few activated effector T-cells, we repeated the experiments from Fig. 2b, but transferring GFP^+CD4^+ Treg isolated from *Foxp3*^{gfp} reporter mice[34] instead using the $CD3^+CD4^+CD25^+$ subset of T-cells. The results show that DSS-treated mice receiving a suboptimal amount of *Drd3*-deficient GFP^+CD4^+ Treg presented a significant improvement of disease manifestation in comparison with those DSS-treated mice receiving *Drd3*-sufficient GFP^+CD4^+ Treg or with those only treated with DSS but without Treg transfer (Fig. S7). Thus, these results (Fig. S7) recapitulate those results obtained in Fig. 2b. To evaluate whether DRD3-signalling in Treg is

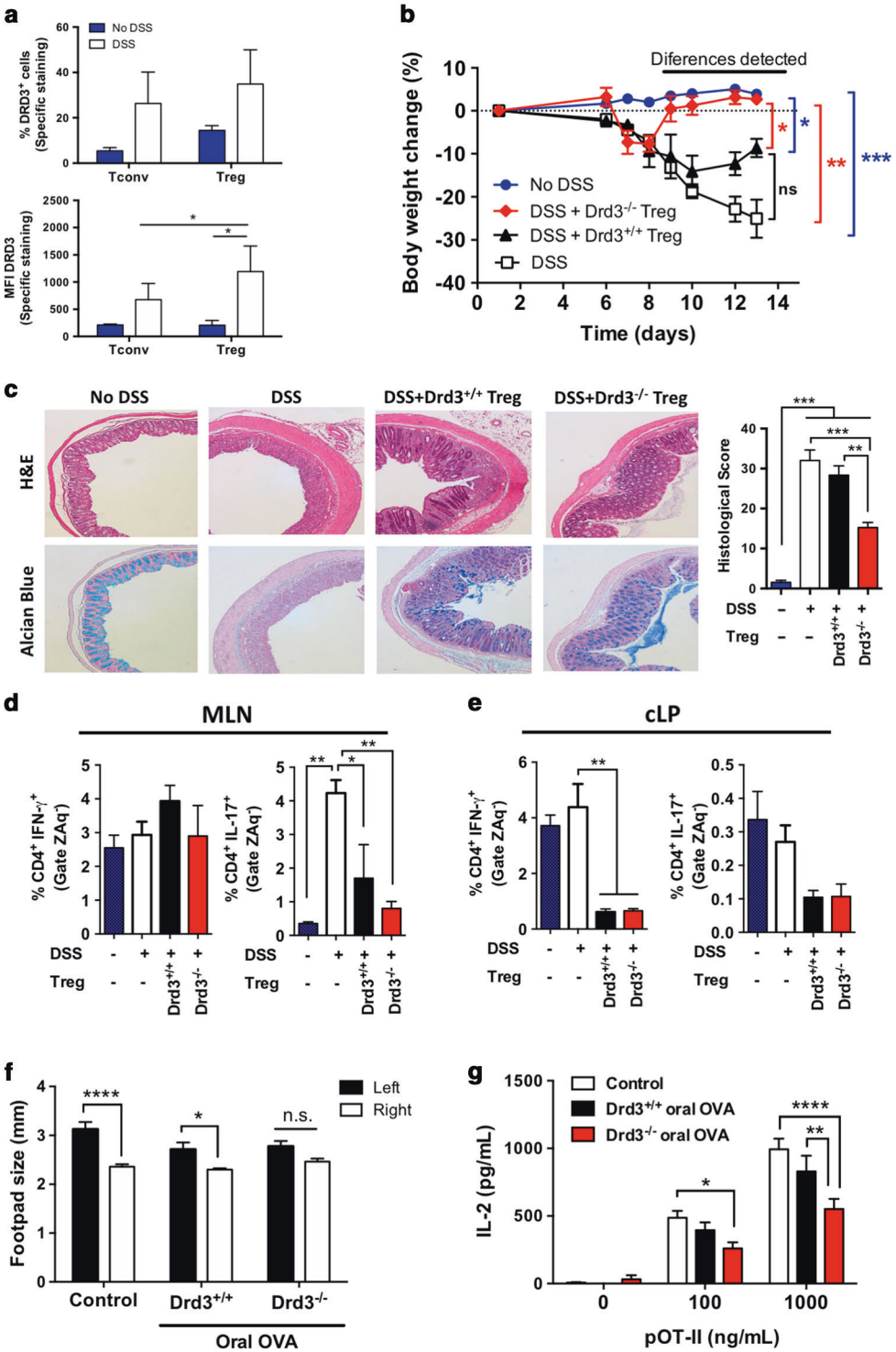

only relevant in conditions of acute inflammation (DSS-induced colitis) or it is also extended to chronic inflammatory colitis, we compared the suppressive potential of Treg from both genotypes in a mouse model of intestinal inflammation induced by the transfer of naïve $CD4^+$ T-cells into lymphopenic mice.[35] For this purpose, naïve ($CD62L^+CD44^-CD25^-$) $CD4^+$ T-cells were isolated from wild-type congenic (*Cd45.2*$^{+/+}$) mice and i.v. transferred into *Rag1*$^{-/-}$ recipient mice. Three weeks later, *Drd3*-sufficient or *Drd3*-deficient Treg cells ($CD4^+GFP^+$) were isolated from *Foxp3*^{gfp} (*Cd45.1*$^{+/+}$) mice and transferred into *Rag1*$^{-/-}$ mice and the disease manifestation was monitored for 10 weeks. The results show that mice receiving *Drd3*-deficient Treg displayed a lower extent of body weight loss than that of mice receiving *Drd3*-sufficient Treg (Fig. S8A). Altogether, these results (Fig. S7 and S8A) reinforce the conclusion that DRD3-signalling in Treg cells plays a relevant pro-inflammatory role favouring the development of both acute or chronic inflammatory colitis.

Since GALT Treg cells play a major role in oral tolerance induction,[36] we wondered whether DRD3-signalling affects the development of oral tolerance using an antigen-specific system.

Fig. 2 *Drd3*-deficient Treg display higher anti-inflammatory activity in vivo. a *Drd3*$^{+/+}$ mice were exposed to normal drinking water or water containing 1.75% DSS during 8 days, and then maintained with normal drinking water for four additional days. MNC were extracted from cLP and surface DRD3 expression was analysed in Treg (ZAq$^-$ CD3$^+$ CD4$^+$ Foxp3$^+$) and Tconv (ZAq$^-$ CD3$^+$ CD4$^+$ Foxp3$^-$) as shown in Fig. S5. Quantification of the percentage (top panel) and MFI (bottom panel) of specific DRD3 immunoreactivity. $n = 6$ mice/group. **b**–**e** Wild-type mice received the i.v. transfer of *Drd3*$^{+/+}$ (black symbols) or *Drd3*$^{-/-}$ (red symbols) Treg cells (CD3$^+$ CD4$^+$ CD25$^+$ cells; 3×10^5 cells/mouse) and then were exposed to 1.75% DSS in the drinking water for 8 days. Afterwards, DSS-containing drinking water was switched to normal water and mice were monitored for 5 additional days. As controls, a group of mice did not receive Treg transfer (white symbols), whilst another group did not receive neither Treg transfer nor DSS (blue symbols). $n = 4$–6 mice/group. **b** Body weight was periodically registered throughout the time course of disease development and the percentage of body weight change relative to initial weight was quantified. The frame of time where differences were found is indicated with a black line. Red brackets and asterisks indicate differences with the red curve, whilst blue brackets and asterisks indicate differences with the blue curve. **c** Histological analysis. Left panel shows representative images of H&E staining (top images) and alcian blue staining (bottom images) of distal colon sections. Right panel shows the quantification of histopathological score. MNC were isolated from the MLN (**d**) or the cLP (**e**) 13 days after Treg transfer and the production of IFN-γ and IL-17A was determined in CD4$^+$ T-cells by intracellular cytokine staining followed by flow cytometry. **f**, **g** *Drd3*$^{+/+}$ or *Drd3*$^{-/-}$ OT-II mice were daily supplemented with PBS (control) or OVA (2.5 mg) via oral during 5 days. One day after the last dose of oral OVA, mice were immunised with a s.c. injection of OVA emulsified with CFA and 7 days later challenged with aggregated OVA in the left hind footpad and PBS in the right hind footpad. **f** Footpad sizes were determined 48 h after the challenge. **g** Splenocytes were cultured in the absence or in the presence of pOT-II (100 or 1000 ng/mL) for 48 h and IL-2 was determined in the culture supernatant by ELISA in triplicates. $n = 8$ mice/group. **a**–**g** Values represent mean ± SEM. *$p < 0.05$; **$p < 0.01$; ***$p < 0.001$; ****$p < 0.0001$ by two-way ANOVA (**a**, **b**, **f** and **g**) or one-way ANOVA (**c**–**e**) followed by Tukey's *post-hoc* test. n.s. no significant differences.

To this end, oral tolerance to OVA was induced in *Drd3*-sufficient and *Drd3*-deficient OT-II mice by feeding them with OVA oral during 5 days. Afterwards, OVA-specific immune response was determined by immunising these mice with OVA s.c. followed by a challenge with aggregated OVA in the footpad one week later. The extent of OVA-specific immune response was determined as the degree of footpad swelling and the potency of T-cell activation in response to pOT-II ex vivo. The results show that OVA oral induced a reduction of footpad swelling in *Drd3*-sufficient OT-II mice, although there was still a significant difference in the size of the challenged footpad (left footpad) in comparison with the control footpad (right footpad). Conversely, no significant differences were observed in the size of control footpad and challenged footpad in *Drd3*-deficient OT-II mice (Fig. 2f). Furthermore, the extent of IL-2 produced by splenocytes in response to pOT-II was lower in *Drd3*-deficient OT-II mice than that produced in *Drd3*-sufficient OT-II mice (Fig. 2g), indicating that *Drd3* deficiency promotes a stronger attenuation of OVA-specific T-cell response. Thus, these results suggest that DRD3-signalling limits the oral tolerance induction.

The selective stimulation of DRD3 attenuates the suppressive activity of Treg by limiting IL-10 production

To address the question of whether DRD3-signalling regulates Treg function, we first compared the suppressive activity of *Drd3*-sufficient and *Drd3*-deficient Treg using an in vitro suppressive assay. Unexpectedly, we did not find any difference in the suppressive activity in these Treg cells (Fig. 3a). As mentioned above, Treg cells isolated from inflamed lamina propria of IBD patients show impaired suppressive activity, nevertheless after isolation they retain their suppressive activity in vitro,[7,8] suggesting that suppressive activity of Treg could be impaired just in situ by mediators produced by the inflamed tissue. Accordingly, we reasoned that suppressive activity of *Drd3*-sufficient Treg should be affected in the presence of DRD3-agonists. To test this possibility, we activated *Drd3*-sufficient Treg in the presence of the selective DRD3 agonist, PD128907, and then assessed their ability to suppress the proliferation of naive CD4$^+$ T-cells in vitro. The results showed that selective stimulation of DRD3 significantly reduced the ability of Treg to suppress CD4$^+$ T-cell proliferation (Fig. 3b), indicating that DRD3-signalling limits Treg function.

To confirm that DRD3-stimulation attenuates Treg suppressive activity using now the natural DRD3 ligand, dopamine, we conducted in vitro suppression assays co-culturing wild-type naïve CD4$^+$ T-cells with *Drd3*-sufficient or *Drd3*-deficient Treg in the presence of low-dopamine levels (100 nM, which stimulates selectively DRD3), such as the situation found in inflamed gut mucosa, or in the presence of high dopamine levels (1000 nM, which stimulates low-affinity and high-affinity DRs), conditions similar to those found in healthy gut mucosa.[10,14] The results show that in the presence of 1000 nM dopamine, both *Drd3*-sufficient or *Drd3*-deficient Treg exert similar suppressive activity attenuating the proliferation of naive CD4$^+$ T-cells (Fig. 3c, d). Nevertheless, in the presence of 100 nM dopamine, the suppressive activity of *Drd3*-sufficient Treg cells was significantly decreased in comparison to *Drd3*-deficient Treg activity. Thus, these results confirm once again that the selective DRD3-stimulation limits Treg suppressive function.

To address the molecular mechanism underlaying the DRD3-mediated attenuation of Treg suppressive activity, we next evaluated how dopamine affected the density of Foxp3 expression, as the decreased expression density of this master transcription factor has been associated to reduced Treg activity and the development of autoimmune disorders.[37] Interestingly, we observed that only when exposed to 100 nM dopamine, but not in the presence of 1000 nM dopamine, the density of Foxp3 expression was significantly reduced (Fig. 3e), thus suggesting that the selective DRD3-stimulation induces a reduction on the density of Foxp3 expression in Treg cells. Because one of the main mechanisms used by Treg to suppress the activity of effector T-cells is the production of IL-10[38], we also tested the possibility that DRD3-signalling regulates IL-10 production by Treg cells. According to the higher suppressive activity observed in *Drd3*-deficient Treg, results obtained from in vitro assays show that *Drd3* deficiency in the presence of dopamine 100 nM resulted in increased production of IL-10 by CD4$^+$CD25$^+$ T-cells (Fig. 3f). To evaluate whether DRD3-signalling affects IL-10 production by Treg in vivo upon gut inflammation, we next analysed IL-10 production in Treg isolated from MLN and cLP obtained from *Drd3*-sufficient and *Drd3*-deficient mice exposed to DSS treatment. The results show that both the frequency of IL-10-producing Treg cells as well as the intensity of IL-10 production by Treg was higher in *Drd3*-deficient Treg lymphocytes in comparison with *Drd3*-sufficient Treg cells (Fig. 3g, h). To evaluate whether, in addition to IL-10, DRD3-signalling affected other molecules involved in Treg suppressive activity, we determined the production of TGF-β and the surface expression of CTLA-4, CD39 and CD73 in Treg of the MLN and cLP obtained from wild-type and knockout mice treated with DSS. The results show that *Drd3* deficiency does not increase the expression of any of these molecules in Treg upon inflammation (Fig. S9). Together, these results indicate that the selective stimulation of DRD3, a situation given in the gut mucosa upon inflammation, limits the suppressive activity of Treg cells by impairing IL-10 production.

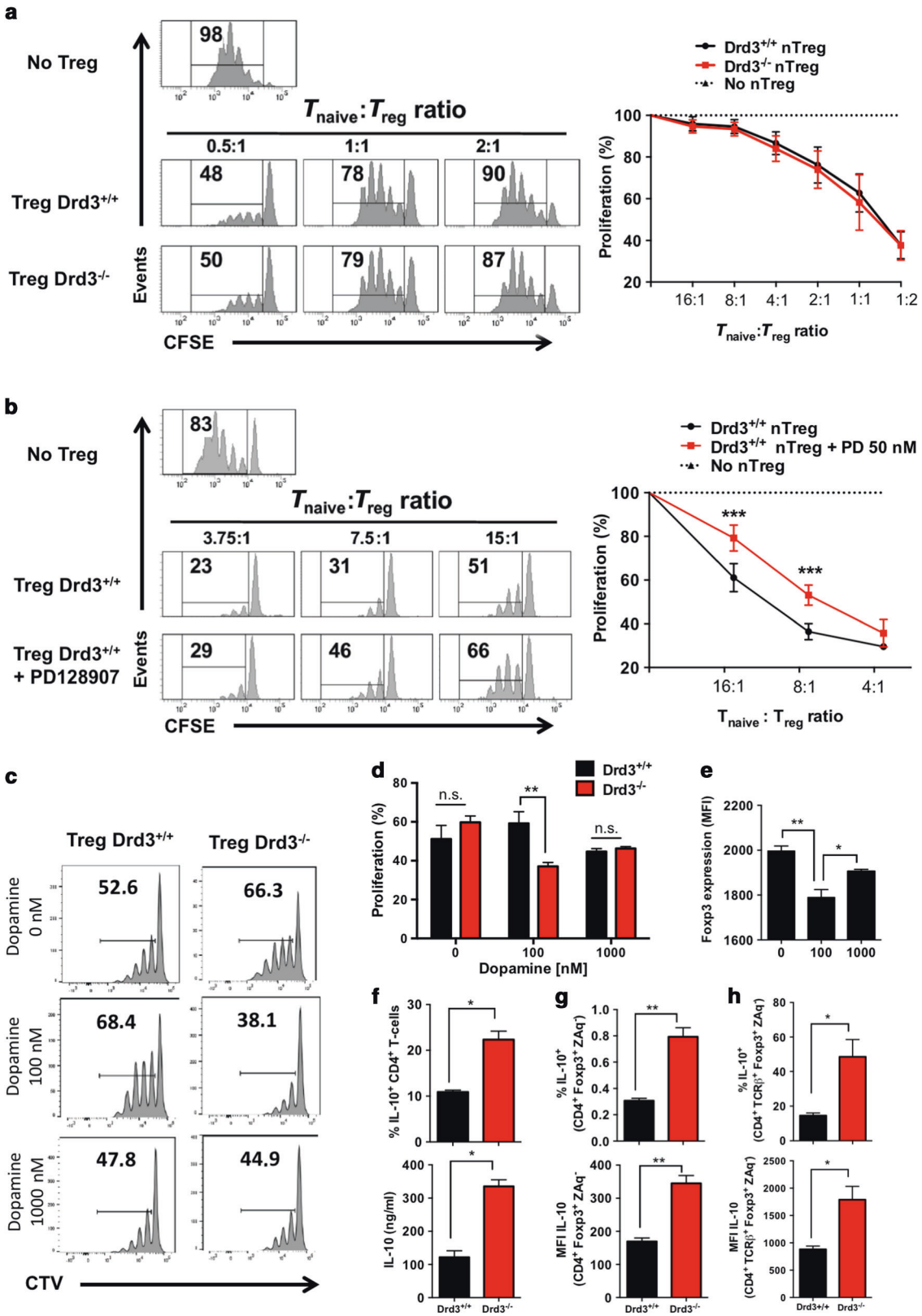

Our results indicate that *Drd3* deficiency provides protection from inflammatory colitis only in *Rag1*-sufficient mice (Fig. 1 and S1). Since the proper function of natural killer cells (NK) and innate lymphoid cells (ILCs) has been shown to depend on RAG activity,[39] we evaluated whether *Drd3* deficiency affects IL-10 production by these cells upon gut inflammation. Accordingly, inflammatory colitis was induced by DSS in $Drd3^{+/+}$ and $Drd3^{-/-}$ mice and, at the peak of disease manifestation, mononuclear cells (MNC) were isolated from the MLN and cLP and IL-10 production was quantified in NK and ILCs. The results show that *Drd3*-deficiency

Fig. 3 DRD3-signalling reduces the suppressive activity and IL-10 production in regulatory T-cells. a, **b** naïve *Drd3*$^{+/+}$ CD45.1^{+} CD45.2^{-} CD4^{+} CD25^{-} T-cells (Tnaive) were loaded with 5 μM CFSE and activated with DCs and anti-CD3 Ab in the presence of CD45.1^{-} CD45.2^{+} Treg (at different Tnaive:Treg ratios). 72 h later, Tnaive proliferation was quantified as the dilution of CFSE-associated fluorescence in the CD45.1^{+} CD45.2^{-} CD4^{+} population by flow cytometry. As a control to determine the maximal Tnaive proliferation, Tnaive were activated in the absence of Treg (No Tregs). **a** Tnaive were co-cultured with freshly isolated *Drd3*$^{+/+}$ or *Drd3*$^{-/-}$ Treg. **b** Prior to the co-culture with Tnaive, *Drd3*$^{+/+}$ Treg were activated with anti-CD3 and anti-CD28 Abs either in the absence or in the presence of the DRD3-selective agonist PD128907 (50 nM) and incubated for 48 h. **a**, **b** In left panels representative histograms of CFSE dilution profiles are shown. Markers show the population of naive T cells displaying CFSE dilution. Numbers on the histograms represent the percentage of naive T cells displaying CFSE dilution. In right panels, the extent of suppression is quantified as the percentage of inhibition of naive T-cells proliferation relative to maximal proliferation (No Treg), where the percentage of suppression is 0 (dotted line). Data from three independent experiments are shown. **c**, **d** naïve *Drd3*$^{+/+}$ CD45.1^{+} CD45.2^{-} CD4^{+} CD25^{-} T-cells (Tnaive) were loaded with 5 μM CTV and activated with anti-CD3 and anti-CD28 Abs and co-cultured with GFP^{+} CD45.1^{-} CD45.2^{+} nTreg (ratio Treg:Tnaive = 1:8) isolated from *Drd3*$^{+/+}$ *Foxp3*^{gfp} or *Drd3*$^{-/-}$ *Foxp3*^{gfp} mice in the presence of 0, 100 or 1000 nM dopamine. After 72 h, the extent of Tnaive proliferation was determined as the dilution of CTV-associated fluorescence in the CD45.1^{+} CD45.2^{-} CD4^{+} population by flow cytometry. **c** Representative histograms of CTV dilution profiles are shown. Markers show the population of Tnaive cells displaying CTV dilution. Numbers on the histograms represent the percentage of Tnaive cells displaying CTV dilution. **d** In right panels, the extent of Tnaive proliferation is quantified. Data from triplicate from a representative of three independent experiments are shown. **e** Treg were isolated from the MLN from *Drd3*$^{+/+}$ *Foxp3*^{gfp} mice and then activated with anti-CD3- and anti-CD28-coated dynabeads (Treg:dynabead ratio = 1:2) in the presence of 0, 100 or 1000 nM dopamine and incubated for 48 h. Foxp3 expression was determined as the MFI associated to GFP. Data from a representative experiment in triplicate are shown. **f** CD4^{+} CD25^{+} T-cells were isolated from *Drd3*$^{+/+}$ or *Drd3*$^{-/-}$ mice, and then activated with anti-CD3- and anti-CD28-coated dynabeads (Treg:dynabead ratio = 1:2) in the presence of dopamine 100 nM for 48 h. Top panel: Treg cells were restimulated with PMA and ionomycin in the presence of brefeldin A, and intracellular IL-10 was immunostained and analysed by flow cytometry. IL-10 production was quantified as the percentage of IL-10^{+} CD4^{+} cells in the ZAq^{+} gate. Bottom panel: IL-10 production was determined in the cell culture supernatant by ELISA. Data from three independent experiments are shown. MNC were isolated from MLN (**g**) or cLP (**h**) of *Drd3*$^{+/+}$ *Foxp3*^{gfp} or *Drd3*$^{-/-}$ *Foxp3*^{gfp} mice treated with 1% DSS. Cells were restimulated ex vivo with PMA and ionomycin in the presence of brefeldin A. IL-10 production was quantified as the percentage (top panels) or MFI (bottom panels) associated to IL-10 immunostaining in Treg. $n = 3$ (**g**) or 4–5 (**h**) mice/group. **a**, **b**, **d**–**h** Values represent mean ± SEM. *$p < 0.05$; **$p < 0.01$; ***$p < 0.001$ by two-way ANOVA (**a**, **b** and **d**) or one-way ANOVA (**e**) followed by Tukey's *post-hoc* test or by unpaired Student's *t* test (**f**–**h**). n.s. no significant differences were found.

induced just a mild reduction on IL-10 production by NK cells or by the global leucocyte population from the MLN (Fig. S10). In addition, no differences were observed in the levels of IL-10 production by NK cells and leucocytes from the cLP or by ILCs from the MLN or the cLP (Fig. S10). Thus, these results rule out the possibility that IL-10 produced by ILCs or NK cells contributes to the different susceptibility of *Drd3*$^{+/+}$ and *Drd3*$^{-/-}$ mice to inflammatory colitis manifestation.

Drd3-deficiency favours the acquisition of gut tropism in Treg cells by enhancing the expression of the C-C chemokine receptor CCR9 The higher attenuation of colitis development exerted by *Drd3*-deficient Treg can be due to two non-excluding possibilities: 1. To a higher suppressive activity, or 2. To an enhanced recruitment of Treg into the gut mucosa. To address the second possibility, we first evaluated the expression of key molecules involved in gut homing, the C-C chemokine receptor CCR9, and the integrin α4β7.[40,41] For this purpose, we isolated Treg cells from MLN of *Drd3*-sufficient and *Drd3*-deficient mice and analysed the expression of CCR9 and α4β7. Importantly, the results show that *Drd3* deficiency resulted in a significant and selective increase of CCR9, both in frequency and density of expression in Treg cells in steady-state (Fig. 4a). Similarly, we observed a higher CCR9 expression in *Drd3*-deficient Treg from the MLN of mice undergoing chronic inflammatory colitis (Fig. S8C, D). Of note, we observed no differences in the expression of Foxp3 between *Drd3*-sufficient and *Drd3*-deficient Treg obtained from the MLN in steady-state (Fig. S11). Interestingly, the increased expression of CCR9 induced by *Drd3* deficiency was also observed in iTregs differentiated from naive CD4^{+} T-cells (Fig. S12).

To determine whether the alteration in the expression of molecules associated to gut tropism induced by *Drd3* deficiency in Treg was also observed in the colonic mucosa upon acute inflammation, we next compared the surface expression of these homing molecules in Treg isolated from the cLP of wild-type or knockout mice in steady-state or upon DSS treatment. Since GPR15 has been involved in colonic tropism of Treg,[42] we also included the expression of this receptor in the analysis. The results show that density of CCR9 expression on colonic Treg was significantly higher in *Drd3*-deficient mice under acute inflammatory conditions, but not in steady-state. Conversely, *Drd3* deficiency induced a lower α4β7 expression in colonic Treg upon DSS treatment (Fig. S13). In addition, we observed no differences in the expression of GPR15 on colonic Treg (Fig. S13), thus ruling out the possibility that DRD3-signalling regulates GPR15 expression.

Afterwards, we wondered whether the higher CCR9 expression observed in *Drd3*-deficient Treg cells is maintained or undergoes changes upon T-cell activation. To address this question, we next isolated Treg cells from the MLN of *Drd3*-sufficient and *Drd3*-deficient mice and they were activated with anti-CD3/anti-CD28 coated dynabeads in the presence of retinoic acid (RA) and IL-2 and the dynamics of CCR9 and α4β7 expression was assessed at different time-points during 7 days. According to the role of RA in imprinting the gut tropism on Treg cells,[43] the expression of both CCR9 and α4β7 was increasing along the time (Fig. 4b). Furthermore, *Drd3*-deficient Treg cells maintained a higher frequency and density of CCR9 expression along the time after T-cell activation up to 7 days. Conversely, α4β7 expression was not affected by *Drd3* deficiency in Treg cells (Fig. 4b). It is noteworthy that the density (MFI) of Foxp3 expression was also similar in *Drd3*-sufficient and *Drd3*-deficient Treg cells isolated from the MLN, both in steady-state (time cero), or after T-cell activation (Fig. 4b, bottom right panel). Next, we attempted to determine whether the selective increase of CCR9 expression induced by *Drd3* deficiency was a general aspect of Treg cells from different locations or it was a particular feature of Treg obtained from MLN. Accordingly, we isolated Treg cells from the spleen of *Drd3*-suffiicient and *Drd3*-deficient mice and then were activated in vitro in the presence of RA and IL-2 and the dynamics of CCR9 and α4β7 expression was assessed at different time points during 7 days. Importantly, the results show that expression of CCR9 and α4β7 was similar in *Drd3*-sufficient and *Drd3*-deficient Treg along the time (Fig. S14), suggesting that the regulation of CCR9 expression exerted by DRD3-signalling seems to be confined to GALT associated Treg cells. Since CCR9 expression is up-regulated by RA,[43] we tested whether the effect of DRD3-

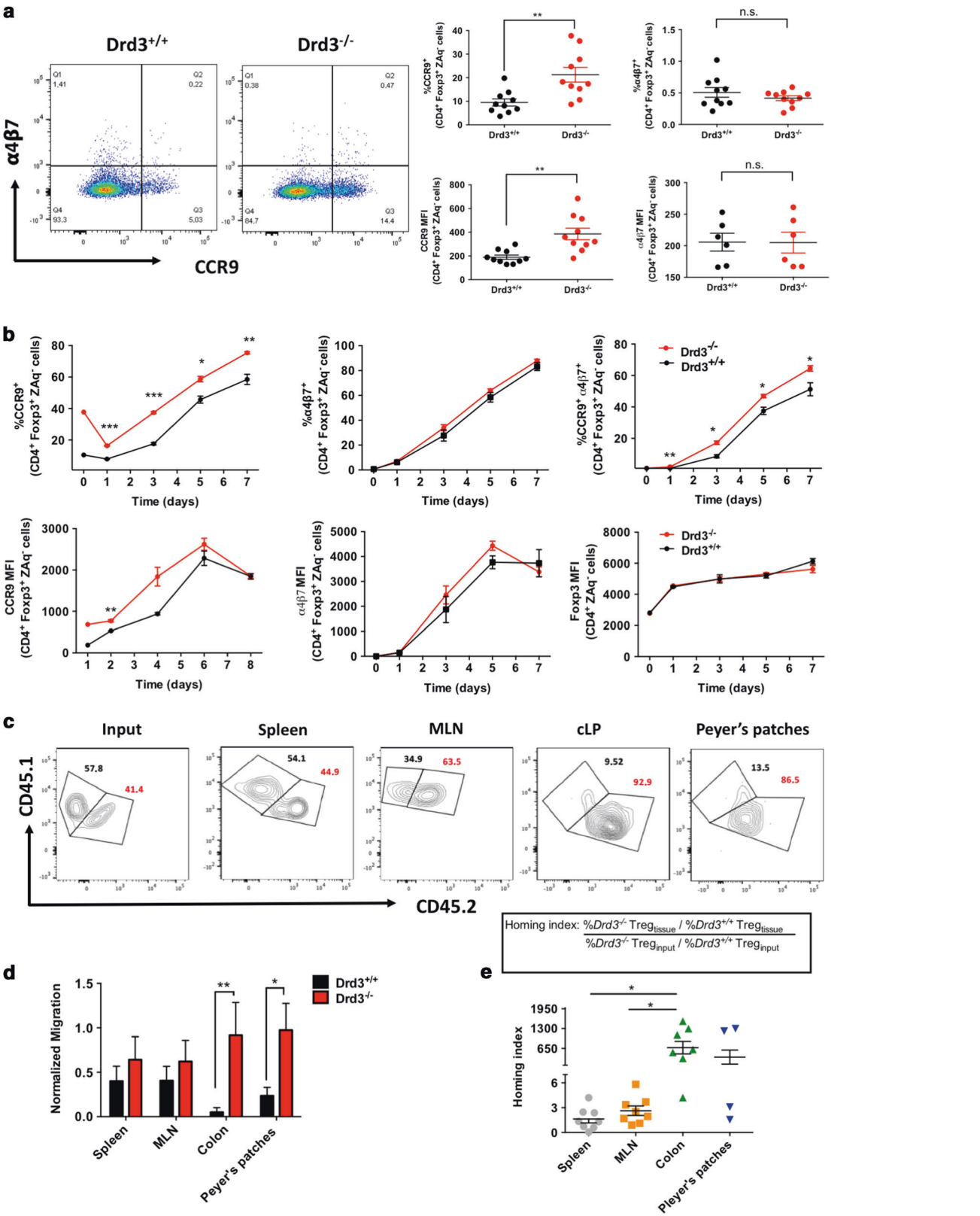

signalling on CCR9 expression was dependent on RA receptor (RAR) stimulation. For this purpose, wild-type or *Drd3*-knockout Treg isolated from the MLN were activated ex vivo in the presence of RA and DRD3-agonists or RAR-antagonist and CCR9 expression was assessed. The results show that RA induced an up-regulation of CCR9 expression (MFI) in *Drd3*-deficient Treg, except when incubated with a RAR-antagonist (Fig. S15). In addition, there was a trend of reduction in the percentage of CCR9 expression in wild-type Treg when treated with a selective DRD3 agonist or dopamine 100 nM, even in the presence of RA (Fig. S15). These

Fig. 4 DRD3-signalling attenuates the recruitment of regulatory T-cells into the gut mucosa upon inflammation. a Treg cells ($CD4^+$ GFP^+) were isolated from MLN of *Drd3*$^{+/+}$ *Foxp3*^{gfp} or *Drd3*$^{-/-}$ *Foxp3*^{gfp} mice and the expression of CCR9 and α4β7 was analysed in the alive (ZAq^-) $CD4^+$ GFP^+ population by flow cytometry. Representative dot plots of CCR9 and α4β7 expression are shown in the left panel. The percentage of cells in the respective quadrants are indicated. In the right panel, CCR9 (left graphs) and α4β7 (right graphs) expression was quantified as the percentage of positive cells (top graphs) or the MFI (bottom graphs). Each symbol represent data obtained from a single mouse ($n = 6$–10 per group). Mean ± SEM are shown. **b** Treg cells ($CD4^+$ GFP^+) isolated from MLN of *Drd3*$^{+/+}$ *Foxp3*^{gfp} or *Drd3*$^{-/-}$ *Foxp3*^{gfp} mice were activated with anti-CD3- and anti-CD28- coated dynabeads (Treg:dynabead ratio = 1:2) in the presence of RA and IL-2 for 7 days. The expression of CCR9 and α4β7 was analysed every other day in the alive (ZAq^-) $CD4^+$ GFP^+ population by flow cytometry. Quantification of the percentage and MFI of CCR9 (left panels), α4β7 (middle panels) expression are shown. Quantification of the frequency of cells expressing both together CCR9 and α4β7 is shown in the top-right panel. Quantification of the density of Foxp3 expression is shown in the bottom-right panel. Values represent mean ± SEM from triplicates. Data from a representative from three independent experiments are shown. **c**–**e** Treg cells ($CD4^+$ GFP^+) isolated from MLN of *Drd3*$^{+/+}$ *Foxp3*^{gfp} (*Cd45.1*$^{+/+}$) and *Drd3*$^{-/-}$ *Foxp3*^{gfp} (*Cd45.1*$^{+/-}$ *Cd45.2*$^{+/-}$) mice were mixed at ratio 1:1 and then i.v. transferred (10^6 total cells per mouse) into wild-type (*Cd45.2*$^{+/+}$) recipients 4 days after initiated the treatment with 1.75% DSS. 24 h later, mice were sacrificed and the arrival of *Drd3*$^{+/+}$ ($CD45.1^+$ $CD45.2^-$) and *Drd3*$^{-/-}$ ($CD45.1^+$ $CD45.2^+$) Treg was analysed in the spleen, MLN, cLP and Peyer's patches by flow cytometry. To normalise the recruitment of transferred Treg to different target tissues, the ratio of *Drd3*$^{+/+}$-to-*Drd3*$^{-/-}$ Treg was analysed before the i.v. transfer (input). **c** Representative contour-plots analysing the expression of CD45.1 versus CD45.2 in the $TCR\beta^+$ $CD4^+$ gated population. The percentage of *Drd3*$^{+/+}$ (black) and *Drd3*$^{-/-}$ (red) Treg are indicated. **d** The extent of migration was determined as the percentage of Treg present in the tissue normalised with the percentage of Treg present in the input (for each genotype). Values represent mean ± SEM; $n = 8$ mice per group. **e** The homing index was calculated as indicated in the top panel. Quantification of the homing index for each target tissue analysed is shown in the bottom panel. Each symbol represents data obtained for a single mouse in the corresponding tissue ($n = 8$). Mean ± SEM are shown. *$p < 0.05$; **$p < 0.01$; ***$p < 0.001$ by unpaired Student's *t* test (**a** and **b**), two-way ANOVA followed by Fisher's *post-hoc* test (**d**) or one-way ANOVA followed by Tukey's *post-hoc* test (**e**). n.s. no significant differences were found.

results suggest that DRD3-mediated down-regulation of CCR9 is independent of RAR-signalling.

To evaluate whether DRD3-mediated regulation of CCR9 expression was confined only to Treg or it was extended to other T-cell subsets, we also evaluated the dynamics of acquisition of gut homing molecules in Tconv isolated from MLN. Interestingly, our results show that *Drd3* deficiency also favours the up-regulation of CCR9 expression in Tconv, although attenuates the acquisition of α4β7 integrin in this subpopulation of T-cells (Fig. S16). In addition, we analysed whether *Drd3* deficiency affected the proliferation and survival of Treg and we observed no significant differences between genotypes (Fig. S17). Interestingly, RA induced a slight decrease in the extent of Treg proliferation in both genotypes (Fig. S17). Altogether, these results indicate that DRD3-signalling attenuates the acquisition of gut tropism in Treg cells found in the MLN.

Since DRD3-signalling has been involved in DCs function,[44] we wondered whether GALT DCs display a higher tolerogenic function in *Drd3*-deficient mice, thus contributing to the attenuated gut inflammation observed in *Drd3*-knockout mice. To address this possibility, DCs isolated from the MLN of *Drd3*-sufficient or *Drd3*-deficient mice were co-cultured with wild-type naïve $CD4^+$ T-cells and the extent of iTreg generation was evaluated 5 days later. The results show that MLN DCs from both genotypes promote iTreg generation in a similar extent (Fig. S18), suggesting that GALT DCs do not contribute to the different severity of inflammatory colitis observed between *Drd3*-deficient and *Drd3*-sufficient mice.

To evaluate whether the resistance to gut inflammation induced by *Drd3* deficiency is actually dependent on CCR9 expression, we next compared how was the manifestation of DSS-induced inflammatory colitis in *Drd3*-deficient, *Ccr9*-deficient and double knockout mice. The results show that wild-type, *Ccr9*-knockout and double knockout mice presented similar disease manifestation, whilst *Drd3*-deficient mice remained refractory to disease manifestation (Fig. S19). Remarkably, these data indicate that resistance to gut inflammation induced by *Drd3* deficiency depends on CCR9 expression.

Lack of DRD3-signalling in Treg increases their recruitment into the gut mucosa upon inflammation

Since *Drd3* deficiency significantly modified gut-tropism in Treg cells, we next sought to evaluate whether DRD3-signalling affects Treg recruitment into the gut mucosa upon inflammatory colitis. To this end, we transferred a mixture of *Drd3*-sufficient and *Drd3*-deficient Treg cells in mice undergoing DSS-induced inflammatory colitis and 24 h later, we traced the destination of Treg cells analysing different tissues by flow cytometry. The results show that the fraction of *Drd3*-deficient Treg was significantly higher than that of *Drd3*-sufficient Treg in the cLP as well as in Peyer's patches (Fig. 4c, d). Conversely, there were no differences in the distribution of *Drd3*-deficient and *Drd3*-sufficient Treg cells in the spleen and MLN (Fig. 4c, d). Furthermore, to reinforce the conclusion that *Drd3* deficiency leads to a differential distribution of Treg cells favouring the recruitment of these cells into the gut mucosa, we also analysed the Homing Index (Fig. 4e, top panel) as described previously.[45] This analysis indicated that *Drd3* deficiency results in an increased recruitment of Treg cells into the cLP in comparison to the spleen and MLN (Fig. 4e, bottom panel). Of note, despite there is a marked trend of higher recruitment of Treg into Peyer's patches led by *Drd3* deficiency, there were no significant differences in the recruitment of *Drd3*-deficient Treg into Peyer's patches in comparison with the spleen and MLN, probably due to the high dispersion of data obtained from Peyer's patches (Fig. 4e, bottom panel). Thus, taken together these results indicate that *Drd3* deficiency leads to enhanced recruitment of Treg into gut mucosa under inflammatory conditions, especially into the cLP.

Targeting *Drd3*-transcription in Treg cells as a therapeutic approach to attenuate the development of inflammatory colitis

Because we observed a strong decrease of DSS-induced colitis manifestation when *Drd3*-deficient Treg were transferred, we next attempted to test the therapeutic potential of targeting DRD3 expression on Treg cells to ameliorate gut inflammation. For this purpose, we generated retroviral vectors codifying for an shRNA directed to reduce *Drd3* transcription (RV-shDrd3), as described previously.[17] Prior to test the therapeutic potential of the inhibition of *Drd3* transcription in Treg cells, we optimised the protocol of Treg transduction (Fig. S20) and confirmed that Foxp3 expression is not changed in Treg cells after transduction with RV-shDrd3 (Fig. S21). Afterwards, we tested the therapeutic effect of Treg cells transduced in optimal condition with RV-shDrd3, which was compared with the effect of Treg cells transduced with control retroviral vectors (RV-Control; codifying just for the reporter gene GFP) in the development of DSS-induced inflammatory colitis. According to the higher IL-10 production observed in the input (Fig. S22), the i.v. transfer of RV-shDrd3-transduced Treg at the beginning of colitis-induction exerted a potent therapeutic effect attenuating disease manifestation in comparison

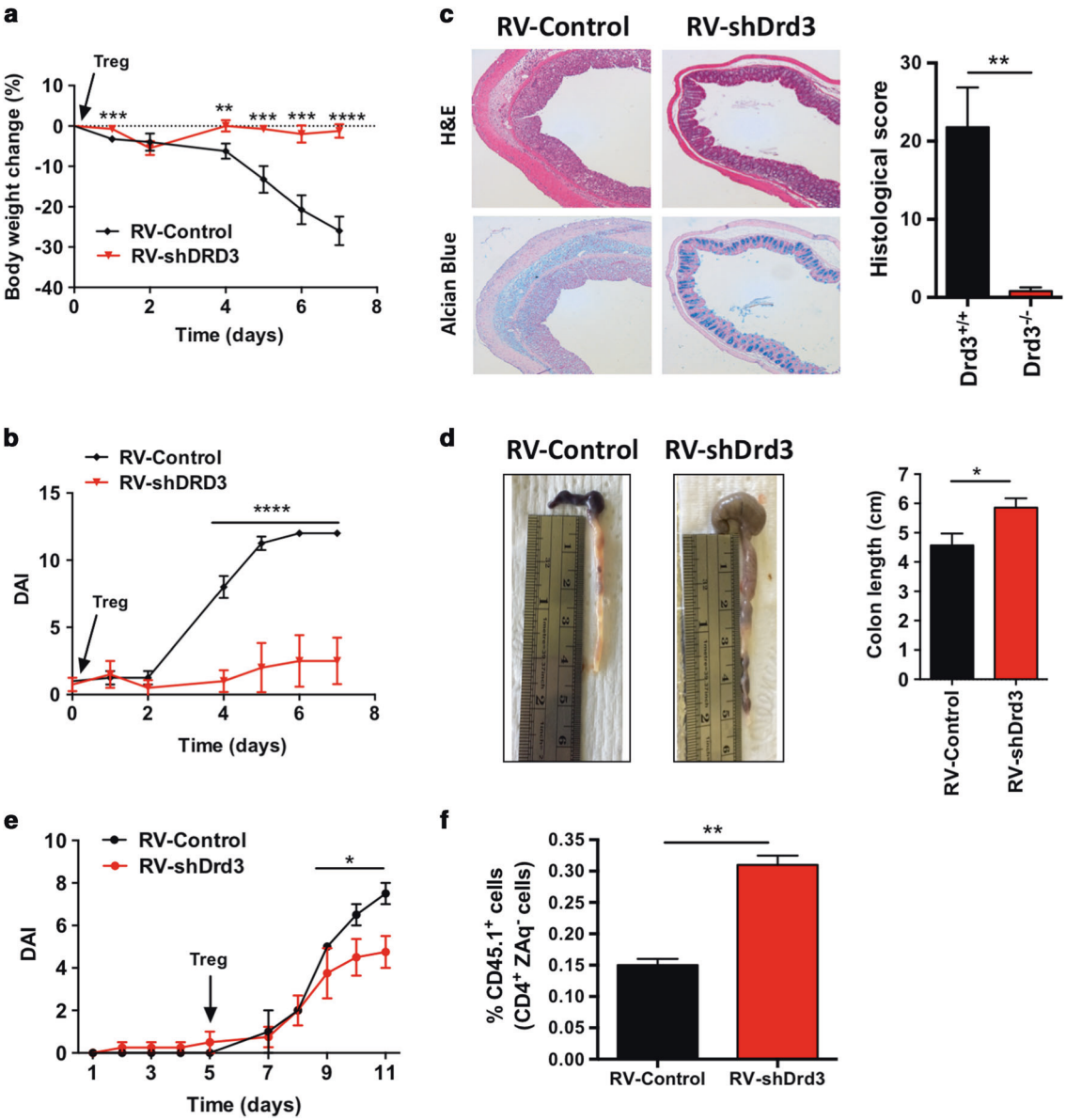

Fig. 5 The transference of Tregs transduced ex vivo with an shRNA for *Drd3* into DSS-treated mice exterts a potent therapeutic effect attenuating the development of inflammatory colitis. a–d Wild-type mice received the i.v. transference of 2×10^5 Tregs and immediately were exposed to 1.75% DSS for 7 days. One group received Treg transduced ex vivo with retroviral particles codifying for a shRNA that attenuates the expression of the Drd3 transcript and GFP as a reporter gene (RV-shDrd3; red symbols), whilst the other group received the transference of Treg transduced ex vivo with retroviral particles encoding only for GFP (RV-Control; black symbols). GFP^+ Treg were purified by cell sorting before transference into recipient mice. **a** Body weight was daily determined and represented as % of body weight change respect to the initial weight. **b** Disease activity index (DAI) was also daily determined, which considers loss of body weight, depositions consistence, and the presence of blood in depositions. **c** Histological analysis. Left panel shows representative images of H&E staining (top images) and alcian blue staining (bottom images) of distal colon sections. Right panel shows the quantification of histopathological score. **d** Length of colons was determined. Left panel shows representative images, whilst right panel shows the quantification. Values are mean ± SEM from 6–8 (**a** and **b**) or 5 (**c** and **d**) mice per group. Data from two independent experiments are shown. **e**, **f** Treg ($Cd45.1^{+/+}$) transduced with RV-shDrd3 (red) or RV-Control (black) as indicated in **a**–**d** were i.v. transferred into wild-type ($Cd45.2^{+/+}$) mice after 5 days of treatment with 1.75% DSS ($n = 4$ mice per group). **e** DAI was daily determined. **f** After 11 days of DSS treatment, mice were sacrificed and the percentage of transferred Treg ($CD45.1^+$) arriving to the cLP was quantified. **a**–**f** $^*P < 0.05$; $^{**}p < 0.01$; $^{****}p < 0.0001$ by unpaired Student's *t* test.

when RV-control-transduced Treg were transferred (Fig. 5a–d). Importantly, the therapeutic effect exerted by RV-shDrd3-transduced Treg cells was observed in multiple parameters, including the attenuation in the loss of body weight (Fig. 5a), decreased disease activity index (DAI; Fig. 5b), reduced alterations in the architecture of gut mucosa (Fig. 5c), and a lesser extent of colon shortening (Fig. 5d). To evaluate the therapeutic potential of RV-shDrd3-transduced Treg at later time-points, when gut inflammation is already triggered, we analysed disease manifestation of DSS-treated mice that received the i.v. transfer of transduced Treg 5 days after the beginning of DSS treatment. The results show that the transfer of RV-shDrd3-transduced Treg reduced the disease severity even when transferred after the initiation of gut inflammation (Fig. 5e). According to the lower disease manifestation observed (Fig. 5e) and to the role of DRD3-signalling attenuating in vivo Treg migration into the colon (Fig. 4c–e), a higher extent of infiltration into the colon was observed for RV-shDrd3-transduced Treg in comparison with

RV-control-transduced Treg (Fig. 5f). Interestingly, the analysis of the input shows that the knock-down of *Drd3* in Treg had no effects in the levels of CCR9 expression (Fig. S22). It is likely that RA contained in the culture to induce Treg differentiation promoted a high CCR9 expression in vitro even in RV-Control transduced Treg. However, it is probable that DRD3-signalling triggered in the inflamed gut mucosa in vivo decreased CCR9 expression, and thereby, reduced the extent of Treg infiltration into the cLP as shown in Fig. 5f. Thus, these results show that the reduction of DRD3 expression in Treg cells exerts a potent therapeutic effect dampening gut inflammation.

DISCUSSION

Recent studies have shown that perturbation of dopamine levels, in tissues that display high dopamine levels upon homoeostatic conditions, is associated with inflammation.[46] Accordingly, the reduction of striatal dopamine levels observed upon neuroinflammation in animal models of Parkinson's disease[47] has been associated with defective stimulation of low-affinity dopamine receptors (DRD1 and DRD2)[20,21] and with the selective stimulation of the high-affinity dopamine receptor DRD3.[48,49] In this regard, DRD1- and DRD2-signalling in astrocytes and microglial cells have been associated with anti-inflammatory effects,[20,21] whereas DRD3-stimulation in these cells has been shown to promote neuroinflammation.[50,51] Similarly, DRD3-signalling in T-cells has been shown to favour neuroinflammation in the context of Parkinson's disease.[19]

Gut inflammation has been also associated with a marked reduction of intestinal dopamine levels in both human IBD patients and mouse models of inflammatory colitis.[14,15] Similar to the case of the striatum in Parkinson's disease, high dopamine levels and the consequent DRD2 stimulation have been associated with decreased gut-inflammation,[31] whilst DRD3-stimulation in T-cells has been described to potentiate effector response mediated by Th1 and Th17 cells, promoting gut inflammation.[17] Nevertheless, despite Treg cells play a fundamental role in maintaining mucosal homoeostasis in the intestine, the effect of perturbations on dopamine levels in Treg function remained unexplored so far.

Since high dopamine levels seem to play a homoeostatic role in dopaminergic tissues, here we attempted to analyse how the reduction of dopamine levels participates in gut inflammation. Our findings show that low-dopamine levels favour the selective stimulation of the high-affinity dopamine receptor DRD3 in regulatory T-cells attenuating their suppressive activity and limiting their recruitment into the gut mucosa. Thus, our study suggests that the reduction in dopamine levels associated to gut-inflammation and the consequent switch in DRs stimulated in mucosal Tregs represents one of the molecular changes responsible of Treg unresponsiveness observed in the gut-mucosa. Moreover, these changes in dopamine levels associated to gut inflammation might explain why the Treg activity is only impaired in situ, but not in vitro.[3] Accordingly, we observed that DRD3-signalling attenuated Treg function in vivo using models of inflammatory colitis (Figs. 1, 2, 5 and S8), and in vitro in the presence of dopamine or a selective DRD3 agonist (Fig. 3b–d), but not in vitro in the absence of DRD3-stimuli (Fig. 3a).

Previous evidence regarding DRs stimulation on Treg has shown that dopamine reduces the suppressive activity of these cells obtained from both human and mouse, with no relevant role for DRD3-signalling in the regulation of Treg function.[13,52] In apparent controversy with these studies, here we found genetic and pharmacologic evidence indicating that the selective stimulation of DRD3 expressed on Treg, results in the inhibition of Treg suppressive function. In this regard, it is likely that the simultaneous stimulation of DRD2 and DRD3 on Treg exerted by the use of the non-selective agonist quinpirole[53] observed by Kipnis et al., has masked the inhibitory effect induced by the exclusive stimulation of DRD3.[52] Conversely, we used here a selective DRD3 agonist that has not previously tested in Treg, PD128907, which display 7-to-54 folds preference by DRD3 over DRD2.[54,55] On the other hand, in the study of Cosentino et al., the contribution of DRD3 in the dopamine-induced inhibition of the suppressive function of Treg was ruled out based on the absence of effect seen upon treatment with a selective DRD3 antagonist.[13] However, is important to note that the antagonist concentration used in that study was below the reported inhibition constant for DRD3.[56] Thus, the present work provides pharmacologic and genetic evidence about dopaminergic regulation of Treg function in vitro and in vivo exerted by DRD3-signalling, an important effect that was previously unappreciated.

To address the mechanism underlying the defective suppressive activity of Treg induced by DRD3-signalling we evaluated how DRD3-stimulation affected the expression/production of molecules involved in the immunosuppressive Treg function, including CTLA-4, CD39, CD73, TGF-β and IL-10. Interestingly, with the only exception of IL-10, none of the molecules evaluated was up-regulated by *Drd3* deficiency in Treg (Fig. S9). We found a selective effect of DRD3-signalling attenuating IL-10 production (Fig. 3f–h), which represents one of the main mechanisms by which Treg limits gut inflammation. Indeed, the genetic deficiency of IL-10 results in spontaneous inflammatory colitis in mice.[38] Of note, IL-10 production by Treg has been described to be dependent on the transcriptional regulator B-lymphocyte-induced maturation protein-1 (Blimp1),[57] whose expression is induced in a cAMP-dependent manner.[58] In this regard, we have previously described that DRD3-signalling in $CD4^+$ T-cells is coupled to the stimulation of $G\alpha_{i/0}$-protein, thus reducing intracellular cAMP levels.[18] Thereby, it is likely that the reduction of IL-10 production induced by DRD3-signalling is mediated by limiting blimp-1 expression in Treg, nevertheless, this possibility should be experimentally validated.

Interestingly, our findings show that DRD3-signalling not only attenuates Treg suppressive function in the intestine, but also their recruitment into the gut mucosa. In this regard, dopamine has been previously associated to changes in the migratory pattern of cells from both the innate and adaptive immune system. For instance, it has been recently described that DRD4-stimulation in human macrophages acts at the epigenetic level in the promoter of *Ccr5*, increasing CCR5 expression and their migratory ability to infiltrate the brain.[59] Conversely, DRD1-signalling was identified as a repressor of CCR5 expression.[59] Accordingly, the depletion of dopamine by the treatment of mice with an inhibitor of dopamine-synthesis, α-methylparatyrosine, exerted a significant reduction in the recruitment of peripheral macrophages into the nigro-striatal pathway in a mouse model of Parkinson's disease.[60] With regard to the role of dopamine in the migratory pattern of the adaptive immune system, Watanabe et al. have shown pharmacologic evidence suggesting that DRD3-signalling potentiates $CD8^+$ T-cell migration towards CCL19, CCL21 and CXCL12 using in vitro transwell assays.[61] According to the role of CCR7 (receptor for CCL19 and CCL21) in the homing of naïve T-cells into lymph nodes across the body, the same authors showed that the systemic administration of a DRD3 antagonist reduced the recruitment of naïve $CD8^+$ T-cells into the lymph nodes.[61] Interestingly, another study has shown pharmacologic evidence suggesting that DRD5-signalling attenuates CCR4 expression in Treg and the consequent recruitment towards CCL22-containing chamber in transwell assays.[52] Here, we provide in vivo evidence using genetic approaches demonstrating that DRD3-signalling in Treg reduces CCR9 expression, thereby dampening their recruitment into the gut mucosa. Altogether these studies indicate that dopamine constitutes a master regulator of leucocyte migration, exerting complex changes in the migration pattern of immune cells, which depends on the precise dopamine levels reached by specific tissues.

CCR9 and α4β7 integrin constitute key homing molecules that lead T-cells into the small intestine mucosa under homoeostatic conditions.[41] However, it has been shown that the production of CCL25, the endogenous CCR9 agonist, is strongly increased in the colonic mucosa upon inflammation.[62] Similarly, the expression of the endogenous α4β7 ligand MadCAM-1 is highly up-regulated in the vascular endothelium of the inflamed colonic mucosa.[63] Thereby, CCR9 and α4β7 drive the trafficking of T-cells into the colonic mucosa in inflammatory colitis. Our results here show that *Drd3* deficiency leads to increased CCR9 expression without affecting α4β7 expression on Treg cells obtained from the MLN, the lymphoid organ where colonic tropism is imprinted (Fig. 4b). Nonetheless, *Drd3* deficiency in Tconv isolated from the MLN resulted in up-regulation of CCR9 but down-regulation of α4β7 (Fig. S16). Thus, this differential regulation of gut homing molecules by DRD3 signalling in Treg and Tconv makes DRD3 a key therapeutic target for the treatment of IBD. In this regard, it is expected that inhibition of DRD3-signalling should increase Treg infiltration but decrease Tconv infiltration into the colonic mucosa upon gut inflammation.

Since CCR9 and α4β7 are not only up-regulated in small intestine inflammation, but also in colon inflammation,[62,64] these homing molecules constitute key molecular targets for both CD and UC. Indeed, several drugs and humanised antibodies directed to inhibit the CCR9-CCL25 and α4β7-MadCAM-1 interactions have been used as therapeutic strategies for CD and UC.[65,66] Nevertheless, these therapeutic approaches attenuate the trafficking not only of Tconv, but also of Treg. Here we present data offering a more attractive molecular target, DRD3, which upon its inhibition selectively improves Treg infiltration into the inflamed gut mucosa. Furthermore, the inhibition of DRD3 would abrogate the inhibitory effect of low-dopamine levels on the suppressive activity of Treg, thus improving the ability of these cells to attenuate gut inflammation. Thereby, the data presented in this study suggest DRD3 as a promising molecular target for IBD and encourage to test the therapeutic potential of the inhibition of DRD3-signalling in CD and UC patients.

METHODS

Mice

Wild-type C57BL/6 (*Drd3*$^{+/+}$; *Cd45.2*$^{+/+}$), *Ccr9*$^{-/-}$ and *Rag1*$^{-/-}$ mice were obtained from The Jackson Laboratory. C57BL/6 *Drd3*$^{-/-}$ mice were kindly donated by Dr. Marc Caron.[67] C57BL/6 *Foxp3*^{gfp} reporter mice generated as described before[34] were obtained from The Jackson Laboratory. Both OT-II and B6.SJL-*Ptprc*^{a} (*Cd45.1*$^{+/+}$) were kindly provided by Dr. María Rosa Bono. *Drd3*$^{-/-}$ OT-II, *Rag1*$^{-/-}$ *Drd3*$^{-/-}$, *Cd45.1*$^{+/-}$ *Cd45.2*$^{+/-}$, *Foxp3*^{gfp} *Drd3*$^{-/-}$ and *Ccr9*$^{-/-}$ *Drd3*$^{-/-}$ (double knockout) mice were generated by crossing parental mouse strains. We confirmed these new strains to be transgenic and *Drd3* deficient or *Ccr9* deficient by flow cytometry analysis of blood cells and PCR of genomic DNA, respectively. Mice from 8 to 10 weeks were used in all experiments.

Reagents

mAbs for flow cytometry: anti-FoxP3 (clone FJK-16S) conjugated to Phycoerythrin (PE)-Cyanine 7 (Cy7) and Allophycocyanin (AlloPC), and anti-IFN-γ (clone XMG1.2) conjugated to PE-Cy7, anti-α4β7 (clone DATK32) conjugated to PE and anti-CCR9 (clone CW.1.2) conjugated to AlloPC or to AlloPC-Cy7 were obtained from eBioscience (San Diego, CA, USA). Anti-CD4 (clone GK1.5) conjugated to AlloPC and AlloPC-Cy7; anti-CD25 (clone PC61) conjugated to FITC; anti-CD44 (clone IM7) conjugated to PE; anti-CD62L (clone MEL14) conjugated to AlloPC-Cy7; anti-IL-17A (clone TC11-181710.1) conjugated to APC; anti-CD45.2 (clone 104) conjugated to PE-Cy7; anti-CD45.1 (clone A20) conjugated to Brilliant Violet (Bv)421; anti-TCRVα2 (clone B20.1) conjugated to PE and TCRVβ5 (clone MR9-4) conjugated to AlloPC were purchased from Biolegend (San Diego, CA, USA). mAbs for Cell Culture: the followings mAbs low in endotoxins and azide free (LEAF) were purchased from Biolegend: anti-CD28 (clone 37.51), anti-CD3ε (clone 145-2C11) and anti-IFN-γ (clone AN-18). Carrier-Free cytokines TGF-β1 and IL-2 were purchased from Biolegend. Zombie Aqua (ZAq) Fixable Viability dye detectable by flow cytometry was purchased from Biolegend. PMA, ionomycin and RA were purchased from Sigma-Aldrich (San Luis, MO, USA). Cell Trace CFSE, Brefeldin A and FBS were obtained from Life Technologies (Carlsbad, CA, USA). The peptide derived from the chicken ovalbumin ($OVA_{323-339;}$ OT-II peptide or pOT-II) was purchased from Genescript (Piscataway, NJ, USA). CFA and anti-CD3/anti-CD28 conjugated dynabeads were purchased from Thermo Scientific. BSA was purchased to Rockland (Limerick, PA, USA). DSS was obtained from MP Biomedicals. DRD3 agonist, PD128907, was purchased from TOCRIS. Cell trace violet (CTV) was obtained from Invitrogen (Carlsbad, CA, USA). All tissue culture reagents were bought from Life Technologies.

$CD4^+$ T-cell isolation, activation and differentiation in vitro

Total $CD4^+$ T-cells were obtained by negative selection of splenocytes according to manufacturer instructions (Miltenyi). Further purification of Treg ($CD4^+CD25^{high}$) and naive $CD4^+$ T-cells ($CD4^+CD62L^+CD44^-CD25^-$) was achieved by labelling enriched $CD4^+$ T-cells with the corresponding antibodies and subsequent cell sorting using a FACS Aria II (BD), obtaining purities over 98%. Purification of Treg cells from *Foxp3*^{gfp} mice was carried out by isolating GFP^+CD4^+ cells by cell sorting. All in vitro experiments were performed using complete RPMI medium (supplemented with 10% FBS, 2 mM L-Glutamine, 100 U/mL Penicillin, 100 µg/mL Streptomycin and 50 µM β-mercaptoethanol). To assess proliferation, Treg or naive $CD4^+$ T-cells were stained with 5 µM CFSE or 5 µM CTV and stimulated for 3 days with 50 ng/well of plate-bound anti-CD3 mAb and 2 µg/mL soluble anti-CD28 mAb on flat-bottom 96-well plates (Thermo Scientific). The extent of T-cell proliferation was determined as the percentage of dilution of CFSE- or CTV-associated fluorescence by flow cytometry.

To induce the differentiation to iTreg, freshly purified naive $CD4^+$ T-cells were activated with anti-CD3 and anti-CD28 mAb (as indicated above) or in the presence of DCs (DCs-to-T-cell ratio of 1:5) and anti-CD3 mAb (1 µg/mL), in the presence of 5 ng/mL TGF-β1, 10 ng/mL IL-2 and 100 nM RA. At different incubation times, the cells were assessed for gene and protein expression.

Flow cytometry

For intracellular cytokine staining analysis, cells were restimulated with 1 µg/mL ionomycin and 50 ng/mL PMA for 4 h, in the presence of 5 µg/mL brefeldin A. Cell surface staining with fluorochrome-coupled primary Ab was carried out in PBS with 2% FBS. For intracellular staining, cells were first stained with ZAq Fixable Viability kit (Biolegend), followed by staining for cell-surface markers and then resuspended in fixation/permeabilization solution (3% BSA and 0.5% saponin in PBS). Samples including the analysis of Foxp3 were resuspended in fixation/permeabilization solution (Foxp3 Fixation/Permeabilization; eBioscience) according to the manufacturer instructions. For DRD3-immunostaining, cells were first incubated for 10 min with rat anti-mouse CD16/32 Ab (1 µg per 100 µL; TrueStain FcX from Biolegend) for blocking non-specific binding of immunoglobulin to the Fc receptors. Afterwards, the rabbit IgG anti-DRD3 primary antibody (ADR-003, Alomone labs) was directly used or pre-incubated with the antigenic peptide $DRD3_{15-29}$ (CGAENSTGVN-RARPH) used to develop the antibody (in a mixture of 0.8 mg/ml of anti-DRD3 antibody and 0.4 mg/ml of peptide) for 30 min as a control to abolish the specific immunostaining. After washing three times with PBS, cells were incubated 30 min at room temperature with the secondary antibody goat anti-rabbit

AlexaFluor488 antibody (1:200). Data were collected with a FACSCanto II (BD) and results were analysed with FACSDiva (BD) and FlowJo software (Tree Star, Ashlan, OR, USA).

Quantitative RT-PCR

Total RNA extracted from cells using the Total RNA EZNA kit (Omega Bio-Tek), was DNase-digested using the TURBO DNA-free kit (Ambion) and 1 µg of RNA was used to synthesise cDNA utilising M-MLV reverse transcriptase, according to manufacturer's instructions (Life Technologies). Quantitative gene expression analysis was performed using Brilliant II SYBR Green QPCR Master Mix (Agilent), according to manufacturer's recommendations. Primers were used at a concentration of 0.5 µM. We used 40 PCR cycles as follows: denaturation 30 s at 95 °C, annealing 30 s at 60 °C and extension 30 s at 72 °C. Expression of target genes was normalised to *Gapdh*. The sequences of the primers used are the following: *Drd3*, sense 5′-GAACTCCTTAAGCCCCACCAT-3′ and antisense 5′-GAAGGCCCCGAGCACAAT-3′; and *Gapdh*, sense 5′-TCCGTGTTCCTACCCCCAATG-3′ and antisense 5′-GAGTGGGAGT TGCTGTTGAAG-3′.

In vitro suppression assays

Treg ($CD4^+CD25^{high}$) obtained from *Cd45.1*$^{+/+}$ mice were activated with 50 ng of plate-bound anti-CD3 and 2 µg/mL soluble anti-CD28 in the absence or presence of 50 nM PD128907 (TOCRIS). After 2 days, activated Treg were washed and serially diluted to incubate with 5×10^4 CFSE-stained naïve $CD45.2^+$ $CD4^+$ T-cells, 10^4 $CD11c^+$ cells obtained by positive selection (Miltenyi) and 1 µg/mL anti-CD3 in round-bottom 96-well plates (Thermo Scientific). 3 days later, the degree of proliferation was assessed in the $CD4^+CD45.2^+$ population by flow cytometry. When indicated, suppression assays were performed with GFP^+CD4^+ Treg isolated from *Foxp3*^{gfp} *Cd45.2*$^{+/+}$ mice. In those cases, $CD45.1^+CD45.2^-CD4^+CD25^-$ naïve T-cells were loaded with 5 µM CTV and activated with plate-bound anti-CD3 mAb (50 ng) and soluble anti-CD28 mAb (2 µg/mL) and co-cultured with Treg either in the absence or in the presence of dopamine (100 nM or 1000 nM; Sigma-Aldrich). After 72 h, the extent of naive T-cell proliferation was determined as the dilution of CFSE- or CTV-associated fluorescence in the $CD45.1^+CD45.2^-CD4^+$ population by flow cytometry.

Suppression of acute colitis induced by DSS

WT recipient mice were i.v. injected with 3×10^5 Treg ($CD4^+CD25^{high}$) 1 day before starting the administration of 1% or 1.75% DSS in the drinking water. DSS was given for a total period of 8 days and then replaced with normal drinking water until the end of the experiment. Body weight was recorded throughout the time-course of disease development. The extent of loss of the initial body weight was used as the main parameter to determine disease severity. In some experiments, disease activity index (DAI) was also determined as a second readout of disease severity. For this purpose, the percentage of loss of body weight, stool consistence and gross bleeding or occult blood in feces were evaluated periodically throughout the time-course of disease development and each of these three parameters were scored with a scale between 0–4, as described before.[68] Thus, DAI scored from 0 (healthy) to 12 (severe colitis). At the end of the experiment, mice were sacrificed to obtain spleen, MLN and cLP. Tissue was digested and homogenised using gentleMACS™ dissociator and then filtered through cell strainers (70 µm pore). To obtain MNC from cLP, cells were separated using centrifugation in percoll.[69] MNC were re-stimulated with PMA and ionomycin in the presence of brefeldin A and different T-cell populations were analysed by flow cytometry. Transverse sections of fixed colon were cut to 5 µm with a cryostat, mounted on xylanized slides, and H&E stained to assess intestinal inflammation by light microscopy, as previously described.[35]

Oral tolerance induction

Drd3$^{+/+}$ or *Drd3*$^{-/-}$ OT-II mice were daily feed with 100 µL of PBS alone or PBS containing 2.5 mg OVA via oral gavage during 5 days as described.[36]

Delayed type hypersensitivity induction

Mice were anesthetized with 3% sevofluorane and then received a s.c. injection of 250 µg OVA emulsified with CFA (200 µl emulsion per mouse) in the tail base as described.[36] After seven days, mice were challenged with 100 µg of aggregated OVA (contained in 50 µl in PBS) injected in the left hind footpad. OVA was aggregated by incubating at 100 °C for 2 min as described.[70] The right hind footpad received 50 µl of PBS (as a control). The thickness of both hind footpads was quantified 48 h later using a caliper. The potency of the DTH response was quantified comparing the thickness of left and right hind footpads. Afterwards, mice were sacrificed and splenocytes were cultured in 96-well plates (10^5 cells per well) in the presence of pOT-II (0, 100 or 1000 ng/mL) for 48 h and IL-2 was evaluated in the culture supernatant as described.[12]

Histological analysis

Mice were sacrificed and the colons were excised. A representative piece of distal colon from each mouse was fixed in 10% formaldehyde and processed for staining with alcian blue and for hematoxylin and eosin (H&E) staining. Blinded histopathologic evaluation of colons was performed considering inflammation, extent of injury, crypt damage and the percentage of tissue involved by Merken Biotech.

Adoptive transfer chronic colitis model

Rag1$^{-/-}$ recipient mice received the i.v. transfer of 3×10^5 naïve ($CD62L^+CD44^-CD25^-$) $CD4^+$ T-cells isolated from wild-type C57BL/6 (*Drd3*$^{+/+}$; *Cd45.2*$^{+/+}$) mice. After 3 weeks,[69] mice received the i.v. transfer of 10^5 Treg cells ($CD4^+$ GFP^+) isolated from mesenteric lymph nodes of *Drd3*$^{+/+}$ *Foxp3*^{gfp} (*Cd45.1*$^{+/+}$) or *Drd3*$^{-/-}$ *Foxp3*^{gfp} (*Cd45.1*$^{+/+}$) mice. The body weight of each animal was recorded weekly. Ten weeks after Treg transfer, mice were sacrificed to obtain spleen, MLN and cLP. Tissue was digested and homogenised using gentleMACS™ dissociator and then filtered through cell strainers (70 µm pore). To obtain MNC from cLP, cells were separated using centrifugation in percoll.[69] The frequency of Treg and CCR9 expression were assessed by flow cytometry.

Retroviral transduction of Treg and naive $CD4^+$ T cells

For silencing *Drd3* expression, we used the retroviral vector pBullet.[71] We inserted a region coding *gfp*, the U6 promoter, an shRNA directed to *drd3* transcript (5′-TGCCCTCTCCTCTTTGG TTTCAACACAAC-3′) and the H1 promoter, into pBullet vector via NcoI and SalI restriction sites (Genscript, *Pisca*taway, NJ). pBullet vector drives the expression of the entire construct by the CMV promoter upstream the NcoI site. This vector was transfected into Phoenix-AMPHO cells. GFP^+ cells were subsequently purified by cell sorting to generate a stable cell line producing retrovirus encoding shRNA for *Drd3* (RV-shDrd3) in the supernatant. As a non-silencing control, we generated Phoenix-AMPHO cells stably secreting in the supernatant retroviral particles codifying only for *gfp* (RV-Control). $CD4^+$ $CD25^{high}$ Treg cells were isolated from *Drd3*$^{+/+}$ mice, and then activated with anti-CD3- and anti-CD28-coated dynabeads (at Tregs:Dynabeads ratio = 1:1) for 48 h. Then, cells were washed and spinoculated with RV-shDrd3-containing or RV-Control-containing supernatants into a retronectin-coated plate (Takara Bio, Japan). Afterwards, cells were incubated with anti-CD3- and anti-CD28- coated dynabeads (Tregs:Dynabeads ratio = 2:1) for 72 h. Transduction was confirmed by GFP expression by flow cytometry.

Statistical analyses

All values are expressed as the mean ± SEM. Statistical analysis were performed with two-tailed Student's *t* test, when comparing only two groups and with one-way ANOVA, when comparing more than two groups (GraphPad Software). To analyse differences in experiments comparing different genotypes and different treatments, two-way ANOVA test was performed. P values < 0.05 were considered significant.

Study approval

All procedures performed in animals were approved by and complied with regulations of the Institutional Animal Care and Use Committee at Fundación Ciencia & Vida.

ACKNOWLEDGEMENTS

We thank Dr. Marc Caron for providing *Drd3*$^{-/-}$ mice, Dr. María Rosa Bono for providing OT-II and B6.SJL-*Ptprc*^{a} mice. We are grateful to Dr. Alvaro Lladser and Dr. Ernesto López for helpful discussions and technical assistance with viral vectors. We also thank Dr. Sebastián Valenzuela for his valuable veterinary assistance in our animal facility and Dr. María José Fuenzalida for her technical assistance in cell sorting. This work was supported by *Programa de Apoyo a Centros con Financiamiento Basal* AFB-170004 (to Fundación Ciencia & Vida) from "Comisión Nacional de Investigación Científica y Tecnológica de Chile (CONICYT)" and by grants FONDECYT-1170093 (to R.P.), from "Fondo Nacional de Desarrollo Científico y Tecnológico de Chile, MJFF-10332.01 and MJFF-15076 (to R.P.) from Michael J. Fox Foundation for Parkinson Research.

AUTHOR CONTRIBUTIONS

R.P. designed the study, V.U., F.C., O.C., C.P. and A.E. conducted experiments, V.U., F.C., O.C. and C.P. acquired data, V.U., F.C. and R.P. analysed data, R.P. wrote the manuscript.

ADDITIONAL INFORMATION

The online version of this article (https://doi.org/10.1038/s41385-020-00354-7) contains supplementary material, which is available to authorized users.

Competing interests: The authors declare that the research was conducted in the absence of any financial or non-financial competing interests with the exception of a pending patent application describing the therapeutic use of DRD3 inhibition as treatment for inflammatory bowel diseases, and which could be construed as a potential conflict of interest. Authors of said patent present in this paper are: V.U., F.C. and R.P.

Publisher's note Springer Nature remains neutral with regard to jurisdictional claims in published maps and institutional affiliations.

REFERENCES

1. Granlund, A. et al. Whole genome gene expression meta-analysis of inflammatory bowel disease colon mucosa demonstrates lack of major differences between Crohn's disease and ulcerative colitis. *PloS ONE* **8**, e56818 (2013).
2. Olsen, T. et al. TH1 and TH17 interactions in untreated inflamed mucosa of inflammatory bowel disease, and their potential to mediate the inflammation. *Cytokine* **56**, 633–640 (2011).
3. Wu, W. et al. Prolactin mediates psychological stress-induced dysfunction of regulatory T cells to facilitate intestinal inflammation. *Gut* **63**, 1883–1892 (2014).
4. Powrie, F. & Mason, D. OX-22high CD4+ T cells induce wasting disease with multiple organ pathology: prevention by the OX-22low subset. *J. Exp. Med* **172**, 1701–1708 (1990).
5. Mair, I. et al. A context-dependent role for alphav integrins in regulatory T cell accumulation at sites of inflammation. *Front. Immunol.* **9**, 264 (2018).
6. Huber, S. et al. Cutting edge: TGF-beta signaling is required for the in vivo expansion and immunosuppressive capacity of regulatory CD4+CD25+ T cells. *J. Immunol.* **173**, 6526–6531 (2004).
7. Saruta, M. et al. Characterization of FOXP3+CD4+ regulatory T cells in Crohn's disease. *Clin. Immunol.* **125**, 281–290 (2007).
8. Maul, J. et al. Peripheral and intestinal regulatory CD4+ CD25(high) T cells in inflammatory bowel disease. *Gastroenterology* **128**, 1868–1878 (2005).
9. Clark, A. & Mach, N. Exercise-induced stress behavior, gut-microbiota-brain axis and diet: a systematic review for athletes. *J. Int. Soc. Sports Nutr.* **13**, 43 (2016).
10. Asano, Y. et al. Critical role of gut microbiota in the production of biologically active, free catecholamines in the gut lumen of mice. *Am. J. Physiol. Gastrointest. Liver Physiol.* **303**, G1288–G1295 (2012).
11. Pacheco, R., Contreras, F. & Zouali, M. The dopaminergic system in autoimmune diseases. *Front. Immunol.* **5**, 117 (2014).
12. Prado, C. et al. Stimulation of dopamine receptor D5 expressed on dendritic cells potentiates Th17-mediated immunity. *J. Immunol.* **188**, 3062–3070 (2012).
13. Cosentino, M. et al. Human CD4+CD25+ regulatory T cells selectively express tyrosine hydroxylase and contain endogenous catecholamines subserving an autocrine/paracrine inhibitory functional loop. *Blood* **109**, 632–642 (2007).
14. Magro, F. et al. Impaired synthesis or cellular storage of norepinephrine, dopamine, and 5-hydroxytryptamine in human inflammatory bowel disease. *Dig. Dis. Sci.* **47**, 216–224 (2002).
15. Magro, F., Fraga, S., Ribeiro, T. & Soares-da-Silva, P. Decreased availability of intestinal dopamine in transmural colitis may relate to inhibitory effects of interferon-gamma upon L-DOPA uptake. *Acta Physiol. Scand.* **180**, 379–386 (2004).
16. Pacheco, R., Prado, C. E., Barrientos, M. J. & Bernales, S. Role of dopamine in the physiology of T-cells and dendritic cells. *J. Neuroimmunol.* **216**, 8–19 (2009).
17. Contreras, F. et al. Dopamine receptor D3 signaling on CD4+ T cells favors Th1- and Th17-mediated immunity. *J. Immunol.* **196**, 4143–4149 (2016).
18. Franz, D. et al. Dopamine receptors D3 and D5 regulate CD4(+)T-cell activation and differentiation by modulating ERK activation and cAMP production. *J. Neuroimmunol.* **284**, 18–29 (2015).
19. Elgueta, D. et al. Dopamine receptor D3 expression is altered in CD4+ T-cells from Parkinson's disease patients and its pharmacologic inhibition attenuates the motor impairment in a mouse model. Front. Immunol. **10**, 981 (2019).
20. Shao, W. et al. Suppression of neuroinflammation by astrocytic dopamine D2 receptors via alphaB-crystallin. *Nature* **494**, 90–94 (2013).
21. Yan, Y. et al. Dopamine controls systemic inflammation through inhibition of NLRP3 inflammasome. *Cell* **160**, 62–73 (2015).
22. Torres-Rosas, R. et al. Dopamine mediates vagal modulation of the immune system by electroacupuncture. *Nat. Med.* **20**, 291–295 (2014).
23. Besser, M. J., Ganor, Y. & Levite, M. Dopamine by itself activates either D2, D3 or D1/D5 dopaminergic receptors in normal human T-cells and triggers the selective secretion of either IL-10, TNFalpha or both. *J. Neuroimmunol.* **169**, 161–171 (2005).
24. Miyazawa, T., Matsumoto, M., Kato, S. & Takeuchi, K. Dopamine-induced protection against indomethacin-evoked intestinal lesions in rats−role of anti-intestinal motility mediated by D2 receptors. *Med. Sci. Monit.* **9**, BR71–BR77 (2003).
25. Magro, F. et al. Dopamine D2 receptor polymorphisms in inflammatory bowel disease and the refractory response to treatment. *Dig. Dis. Sci.* **51**, 2039–2044 (2006).
26. Corridoni, D., Chapman, T., Ambrose, T. & Simmons, A. Emerging mechanisms of innate immunity and their translational potential in inflammatory bowel disease. *Front. Med.* **5**, 32 (2018).
27. Gerner, R. R. et al. NAD metabolism fuels human and mouse intestinal inflammation. *Gut* **67**, 1813–1823 (2018).
28. Sainathan, S. K. et al. Granulocyte macrophage colony-stimulating factor ameliorates DSS-induced experimental colitis. *Inflamm. Bowel Dis.* **14**, 88–99 (2008).
29. Moraga-Amaro, R., Gonzalez, H., Pacheco, R. & Stehberg, J. Dopamine receptor D3 deficiency results in chronic depression and anxiety. *Behav. Brain Res.* **274**, 186–193 (2014).
30. McKenna, F. et al. Dopamine receptor expression on human T- and B-lymphocytes, monocytes, neutrophils, eosinophils and NK cells: a flow cytometric study. *J. Neuroimmunol.* **132**, 34–40 (2002).
31. Vidal, P. M. & Pacheco, R. Targeting the dopaminergic system in autoimmunity. J. Neuroimmune Pharmacol. **15**, 57–73 (2019).
32. Ueno, A. et al. Th17 plasticity and its relevance to inflammatory bowel disease. *J. Autoimmun.* **87**, 38–49 (2018).
33. Owaga, E. et al. Th17 cells as potential probiotic therapeutic targets in inflammatory bowel diseases. *Int. J. Mol. Sci.* **16**, 20841–20858 (2015).
34. Fontenot, J. D. et al. Regulatory T cell lineage specification by the forkhead transcription factor foxp3. *Immunity* **22**, 329–341 (2005).
35. Ostanin, D. V. et al. T cell transfer model of chronic colitis: concepts, considerations, and tricks of the trade. *Am. J. Physiol. Gastrointest. Liver Physiol.* **296**, G135–G146 (2009).
36. Cassani, B. et al. Gut-tropic T cells that express integrin alpha4beta7 and CCR9 are required for induction of oral immune tolerance in mice. *Gastroenterology* **141**, 2109–2118 (2011).
37. Wan, Y. Y. & Flavell, R. A. Regulatory T-cell functions are subverted and converted owing to attenuated Foxp3 expression. *Nature* **445**, 766–770 (2007).

38. Rubtsov, Y. P. et al. Regulatory T cell-derived interleukin-10 limits inflammation at environmental interfaces. *Immunity* **28**, 546–558 (2008).
39. Karo, J. M., Schatz, D. G. & Sun, J. C. The RAG recombinase dictates functional heterogeneity and cellular fitness in natural killer cells. *Cell* **159**, 94–107 (2014).
40. Johansson-Lindbom, B. et al. Selective generation of gut tropic T cells in gut-associated lymphoid tissue (GALT): requirement for GALT dendritic cells and adjuvant. *J. Exp. Med.* **198**, 963–969 (2003).
41. Mora, J. R. et al. Selective imprinting of gut-homing T cells by Peyer's patch dendritic cells. *Nature* **424**, 88–93 (2003).
42. Kim, S. V. et al. GPR15-mediated homing controls immune homeostasis in the large intestine mucosa. *Science* **340**, 1456–1459 (2013).
43. Iwata, M. et al. Retinoic acid imprints gut-homing specificity on T cells. *Immunity* **21**, 527–538 (2004).
44. Figueroa, C. et al. Inhibition of dopamine receptor D3 signaling in dendritic cells increases antigen cross-presentation to CD8+ T-cells favoring anti-tumor immunity. *J. Neuroimmunol.* **303**, 99–107 (2017).
45. Villablanca, E. J. & Mora, J. R. Competitive homing assays to study gut-tropic t cell migration. *J. Vis. Exp.* **1**, 2619 (2011).
46. Pacheco, R. Targeting dopamine receptor D3 signalling in inflammation. *Oncotarget* **8**, 7224–7225 (2017).
47. Brochard, V. et al. Infiltration of CD4+ lymphocytes into the brain contributes to neurodegeneration in a mouse model of Parkinson disease. *J. Clin. Invest.* **119**, 182–192 (2009).
48. Gonzalez, H. et al. Dopamine receptor D3 expressed on CD4+ T cells favors neurodegeneration of dopaminergic neurons during Parkinson's disease. *J. Immunol.* **190**, 5048–5056 (2013).
49. Chen, Y. et al. Dopamine receptor 3 might be an essential molecule in 1-methyl-4-phenyl-1,2,3,6-tetrahydropyridine-induced neurotoxicity. *BMC Neurosci.* **14**, 76 (2013).
50. Elgueta, D. et al. Pharmacologic antagonism of dopamine receptor D3 attenuates neurodegeneration and motor impairment in a mouse model of Parkinson's disease. *Neuropharmacology* **113**(Pt A), 110–123 (2017).
51. Montoya, A. et al. Dopamine receptor D3 signalling in astrocytes promotes neuroinflammation. *J. Neuroinflammation* **16**, 258 (2019).
52. Kipnis, J. et al. Dopamine, through the extracellular signal-regulated kinase pathway, downregulates CD4+CD25+ regulatory T-cell activity: implications for neurodegeneration. *J. Neurosci.* **24**, 6133–6143 (2004).
53. Burris, K. D. et al. Lack of discrimination by agonists for D2 and D3 dopamine receptors. *Neuropsychopharmacol. Off. Publ. Am. Coll. Neuropsychopharmacol.* **12**, 335–345 (1995).
54. Pugsley, T. A. et al. Neurochemical and functional characterization of the preferentially selective dopamine D3 agonist PD 128907. *J. Pharm. Exp. Ther.* **275**, 1355–1366 (1995).
55. Sautel, F. et al. A functional test identifies dopamine agonists selective for D3 versus D2 receptors. *Neuroreport* **6**, 329–332 (1995).
56. Merlo, S., Canonico, P. L. & Sortino, M. A. Distinct effects of pramipexole on the proliferation of adult mouse sub-ventricular zone-derived cells and the appearance of a neuronal phenotype. *Neuropharmacology* **60**, 892–900 (2011).
57. Cretney, E. et al. Characterization of Blimp-1 function in effector regulatory T cells. *J. Autoimmun.* **91**, 73–82 (2018).
58. Zhang, S. Y. et al. Adrenomedullin 2 improves early obesity-induced adipose insulin resistance by inhibiting the class II MHC in adipocytes. *Diabetes* **65**, 2342–2355 (2016).
59. Basova, L. et al. Dopamine and its receptors play a role in the modulation of CCR5 expression in innate immune cells following exposure to Methamphetamine: Implications to HIV infection. *PloS ONE* **13**, e0199861 (2018).
60. Espinosa-Oliva, A. M. et al. Role of dopamine in the recruitment of immune cells to the nigro-striatal dopaminergic structures. *Neurotoxicology* **41**, 89–101 (2014).
61. Watanabe, Y. et al. Dopamine selectively induces migration and homing of naive CD8+ T cells via dopamine receptor D3. *J. Immunol.* **176**, 848–856. (2006).
62. Trivedi, P. J. et al. Intestinal CCL25 expression is increased in colitis and correlates with inflammatory activity. *J. Autoimmun.* **68**, 98–104 (2016).
63. Souza, H. S., Elia, C. C., Spencer, J. & MacDonald, T. T. Expression of lymphocyte-endothelial receptor-ligand pairs, alpha4beta7/MAdCAM-1 and OX40/OX40 ligand in the colon and jejunum of patients with inflammatory bowel disease. *Gut* **45**, 856–863 (1999).
64. Rivera-Nieves, J. et al. Antibody blockade of CCL25/CCR9 ameliorates early but not late chronic murine ileitis. *Gastroenterology* **131**, 1518–1529 (2006).
65. Biswas, S., Bryant, R. V. & Travis, S. Interfering with leukocyte trafficking in Crohn's disease. *Best. Pr. Res Clin. Gastroenterol.* **38–39**, 101617 (2019).
66. Sands, B. E. Leukocyte anti-trafficking strategies: current status and future directions. *Digestive Dis.* **35**, 13–20 (2017).
67. Joseph, J. D. et al. Dopamine autoreceptor regulation of release and uptake in mouse brain slices in the absence of D(3) receptors. *Neuroscience* **112**, 39–49 (2002).
68. Chen, Y. et al. Induction of experimental acute ulcerative colitis in rats by administration of dextran sulfate sodium at low concentration followed by intracolonic administration of 30% ethanol. *J. Zhejiang Univ. Sci. B* **8**, 632–637 (2007).
69. Menning, A. et al. Retinoic acid-induced gut tropism improves the protective capacity of Treg in acute but not in chronic gut inflammation. *Eur. J. Immunol.* **40**, 2539–2548 (2010).
70. Stransky, B., Faria, A. M. & Vaz, N. M. Oral tolerance induction with altered forms of ovalbumin. *Braz. J. Med Biol. Res* **31**, 381–386 (1998).
71. Weijtens, M. E., Willemsen, R. A., Hart, E. H. & Bolhuis, R. L. A retroviral vector system 'STITCH' in combination with an optimized single chain antibody chimeric receptor gene structure allows efficient gene transduction and expression in human T lymphocytes. *Gene Ther.* **5**, 1195–1203 (1998).